*The following are class notes for a graduate course in introductory Underwater Acoustics presented in the Physics Department, University of Auckland 2002 - 2010.*

*C. T. Tindle* *c.tindle@auckland.ac.nz* *March 2017*

**Contents**

## INTRODUCTION

## DEEP WATER SOUND PROPAGATION

### Speed of sound

The speed of sound at a point in the ocean depends on the static pressure, temperature and salinity. Salinity is fairly constant in deep water away from ice and rivers so salinity changes are not important for sound propagation.

Static pressure increases with depth as

$P = P_o + \rho g z$ where $P_o$ is atmospheric pressure ($10^5$ Pa) and g is the acceleration of gravity (9.8 $m/s^2$)

The density $\rho$ is 1028 $kg/m^3$ and is assumed constant. It does however increase slightly with depth. [The ocean surface would be 30 m higher if water was incompressible.]

Sound speed increases with pressure and therefore with depth.

Sound speed also increases with temperature. In most of the ocean the water is warmest at the surface decreasing to about 1.5 - 2 $^oC$ beyond about 3000 m depth. Seasonal heating only affects the first 100-200 m.

The combined effect of temperature decreasing to a constant and pressure steadily increasing means that in most of the deep ocean there is a sound speed minimum of about 1485 m/s at a depth of about 1000 m.

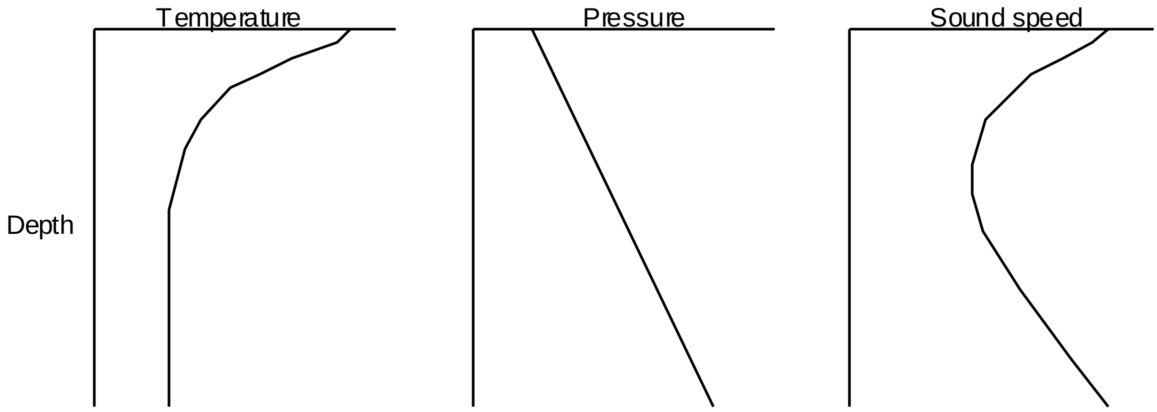


Sound speed at the ocean surface is 1508 $m/s^2$ for a temperature of 15$^o$C.

The range of variation of sound speed of 1485 - 1525 is only about 3% of the actual sound speed but it has important consequences for the propagation of sound.

### SOFAR channel

In most deep water there is a minimum of sound speed at a depth of about 1000 m. This minimum is the SOFAR axis. Sound can become trapped in the SOFAR channel and propagate to long ranges with little attenuation. SOFAR stands for Sound Fixing and Ranging as the discovery of the SOFAR channel led to speculation that it could be used to pinpoint the location of shipping.

### Polar waters

In polar waters the water temperature varies very little with depth and so the sound speed variation is due only to the pressure. The sound speed therefore is minimum at the surface and increases linearly with depth.

The transition from temperate to polar waters is gradual and the minimum of sound speed gradually approaches the surface as latitude is increased.

## Wavefronts and Rays

The change of sound speed leads to refraction of wavefronts of sound. Wavefronts become closer together when the sound speed decreases, leading to bending of the sound waves towards lower sound speed. This refraction leads to trapping of sound in the SOFAR channel.

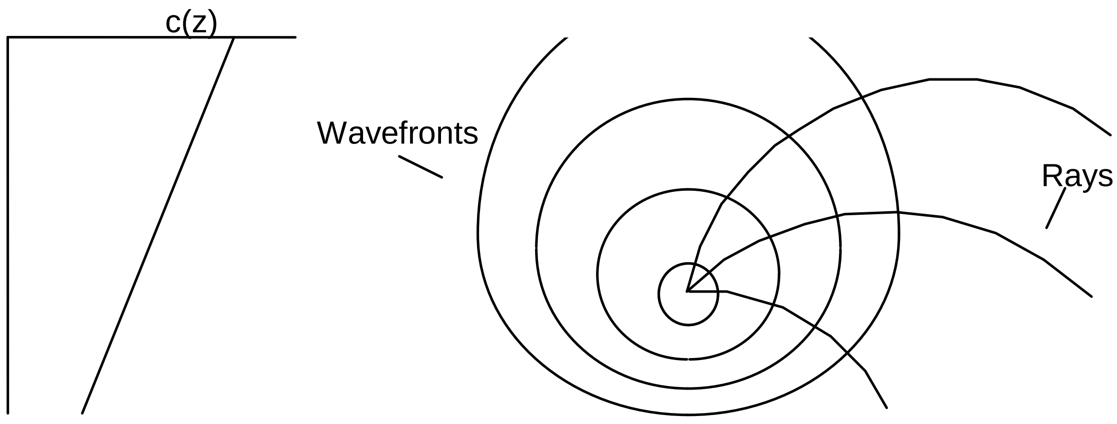


Rays curve towards the minimum of sound speed. In deep water they cycle up and down about the sound speed minimum.

The figures shows ray traces in a profile with a sound speed minimum at 1000 m depth. The source depths are 1000 m and 500 m.

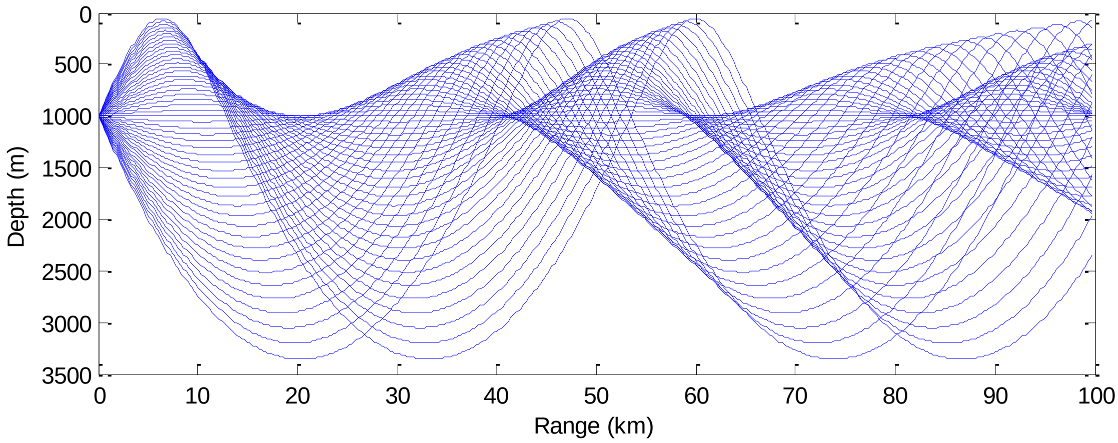


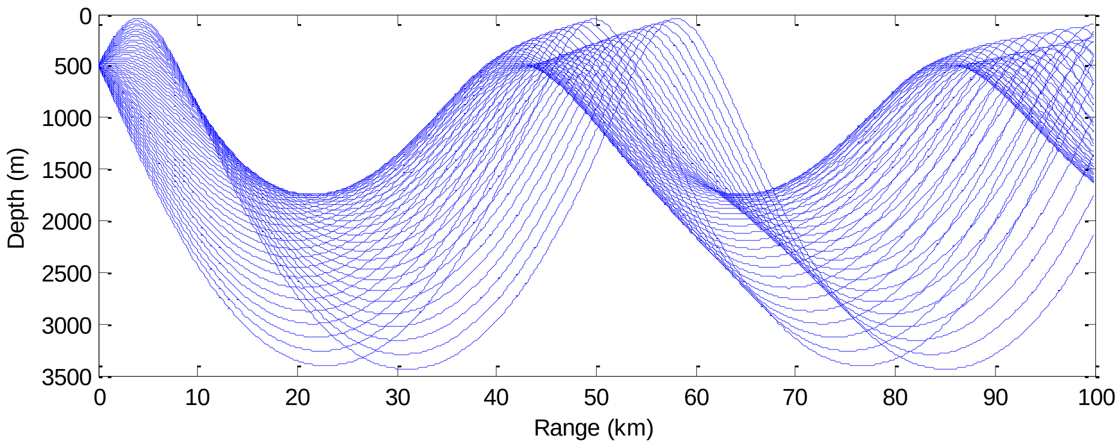

# 1. WAVE EQUATION FOR SOUND WAVES IN A FLUID

**Acoustic pressure** p is the change in pressure associated with the acoustic disturbance.

$$p = P \text{ (instantaneous total pressure)} - P_0 \text{ (average pressure)}$$

For most problems p, $\Delta\rho$ (change in density) are small and second order terms can be neglected.

**Bulk modulus B**

$$B = \frac{\text{stress}}{\text{strain}} = \frac{\text{excess pressure}}{\text{fractional change in volume}}$$

$$B = \frac{p}{-\dfrac{\delta V}{V_0}} \qquad (1.1)$$

This provides the restoring force for vibrational wave motion.

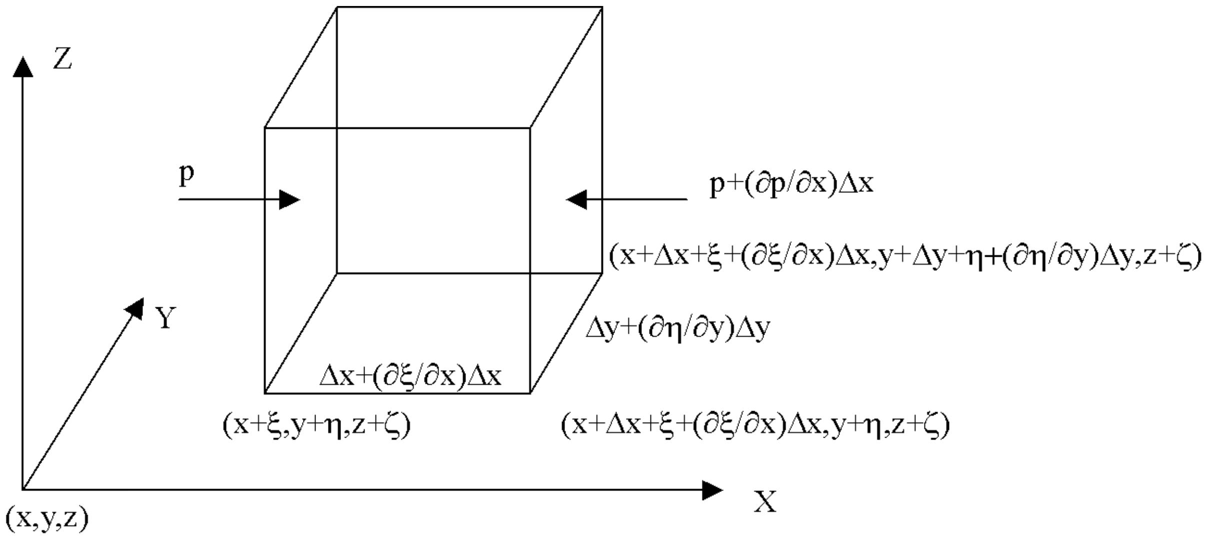


Point (x,y,z) is equilibrium position.

**d** = $(\xi,\eta,\zeta)$ is displacement from equilibrium [$\xi,\eta,\zeta$ are functions of x,y,z,t.]

$\Delta x$, $\Delta y$, $\Delta z$ are sides of box at equilibrium position.

$V_0 = \Delta x\, \Delta y\, \Delta z$ = volume of box at equilibrium position.

Change in volume = $[\Delta x + (\partial\xi/\partial x)\,\Delta x]\,[\Delta y + (\partial\eta/\partial y)\,\Delta y]\,[\Delta z + (\partial\zeta/\partial z)\,\Delta z] - \Delta x\,\Delta y\,\Delta z$

$$\delta V = [\, \partial\xi/\partial x + \partial\eta/\partial y + \partial\zeta/\partial z \,]\, \Delta x\, \Delta y\, \Delta z$$

=> $\delta V/V_0 = \text{div}\, \mathbf{d}$

and from (1)

$$p = -B \,\mathrm{div}\, \mathbf{d} \qquad (1.2)$$

**Newton's Laws**

Total force in X direction $= [-(\partial p/\partial x)\,\Delta x]\,\Delta y\,\Delta z$

Using $\Sigma F = ma$

$$-(\partial p/\partial x)\,\Delta x\,\Delta y\,\Delta z = \rho\,\Delta x\,\Delta y\,\Delta z\,(\partial^2\xi/\partial t^2)$$

In three dimensions

$$-\,\mathrm{grad}\, p = \rho\,(\partial^2\mathbf{d}/\partial t^2) \qquad (1.3)$$

Take div

$$-\,\mathrm{div}\,\mathrm{grad}\, p = \rho\,[\partial^2(\mathrm{div}\,\mathbf{d})/\partial t^2]$$

=> $-\nabla^2 p = -(\rho/B)\,(\partial^2 p/\partial t^2)$

=> $\nabla^2 p = (1/c^2)\,(\partial^2 p/\partial t^2)$ (1.4)

where $c^2 = B/\rho$

**Wave Equation**

Equation (1.4) can be written

$$\nabla^2 p = (1/c^2)\,(\partial^2 p/\partial t^2) \qquad (1.5)$$

which is the wave equation for small amplitude sound propagation.

If a harmonic source with time dependence $\exp(-i\omega t)$ is assumed, the pressure will also have time dependence $\exp(-i\omega t)$ and we obtain the **Helmholtz Equation**

$$\nabla^2 p + (\omega/c)^2\, p = 0 \qquad (1.6)$$

**Displacement potential** $\phi_d$

Define

$$\mathbf{d} = -\,\mathrm{grad}\,\phi_d \qquad (1.7)$$

From (1.2)

$$p = B\,\nabla^2\phi_d \qquad (1.8)$$

Substitute in (1.4)

$$\nabla^2\phi_d = (1/c^2)\,(\partial^2\phi_d/\partial t^2) \qquad (1.9)$$

i.e. $\phi_d$ satisfies the wave equation.

Displacement potential is important for describing sound in solids because pressure has no meaning in a solid and the scalar $\phi_d$ is easier to use than the vector **d**.

## 2. RAY MODELLING

The wave equation for a harmonic (i.e. single frequency) source can be written

$$\nabla^2 p + k^2 p = 0 \qquad (2.1)$$

where $\nabla^2 = \partial^2/\partial x^2 + \partial^2/\partial y^2 + \partial^2/\partial z^2$

p is the acoustic pressure, $k = \omega/c$ is the wave number and the sound speed c is a function of position i.e c(x,y,z).

Consider a solution of the form $p = A\, e^{i\phi}$ where A is a slowly varying amplitude and $\phi$ is a phase. Surfaces of constant $\phi$ all have the same phase i.e. they are wavefronts.

Substituting and separating real and imaginary parts gives

$$\nabla^2 A - [(\partial\phi/\partial x)^2 + (\partial\phi/\partial y)^2 + (\partial\phi/\partial z)^2]\, A + k^2 A = 0$$

and

$$2\, \nabla A . \nabla\phi + A\, \nabla^2\phi = 0$$

Now assume $\nabla^2 A/A << k$ i.e. the amplitude is slowly varying to obtain

$$(\partial\phi/\partial x)^2 + (\partial\phi/\partial y)^2 + (\partial\phi/\partial z)^2 = k^2 \qquad (2.2)$$

Now $\phi$ = constant is a wavefront and the vector grad($\phi$) = $(\partial\phi/\partial x, \partial\phi/\partial y, \partial\phi/\partial z)$ is normal to the wavefront.

If s is the path length along a ray an element **ds** = (dx, dy, dz) is also normal to the wave front. Therefore

$$dx/ds = (\partial\phi/\partial x)/[(\partial\phi/\partial x)^2 + (\partial\phi/\partial y)^2 + (\partial\phi/\partial z)^2]^{1/2}$$

where the denominator ensures that $dx^2 + dy^2 + dz^2 = ds^2$ as required.

Hence using Eq. (2.2) we obtain

$$dx/ds = (1/k)\, (\partial\phi/\partial x) \qquad (2.3)$$

We can now eliminate $\phi$ by noting

$$d\phi/ds = (\partial\phi/\partial x)(dx/ds) + (\partial\phi/\partial y)(dy/ds) + (\partial\phi/\partial z)(dz/ds)$$

$$= k\, (dx/ds)(dx/ds) + k\, (dy/ds)(dy/ds) + k\, (dz/ds)(dz/ds) \qquad \text{using (2.3)}$$

$$= k$$

This shows that the derivative of the phase as a function of distance perpendicular to the wavefront is equal to the wave number as expected.

Now take $\partial/\partial x$ to give

$$\partial/\partial x(d\phi/ds) = \partial k/\partial x$$

=> $$d/ds(\partial\phi/\partial x) = \partial k/\partial x$$

=> $$d/ds(k\,dx/ds) = \partial k/\partial x \qquad \text{using (2.3)}$$

Finally using $k = \omega/c$ with $c(x,y,z)$ we obtain

$$\frac{d}{ds}\left(\frac{1}{c}\frac{dx}{ds}\right) = \frac{\partial}{\partial x}\left(\frac{1}{c}\right) \tag{2.4}$$

This equation leads to ray tracing.

**Ray Solutions**

Consider $c = c(z)$ i.e a function of depth only.

$$(d/ds)[(1/c)(dx/ds)] = 0$$

=> $$(1/c)(dx/ds) = \text{constant}$$

Similarly

$$(1/c)(dy/ds) = \text{constant}$$

=> $$dy/dx = \text{constant}$$

Therefore propagation is confined to a plane. Assume it is $y = 0$.

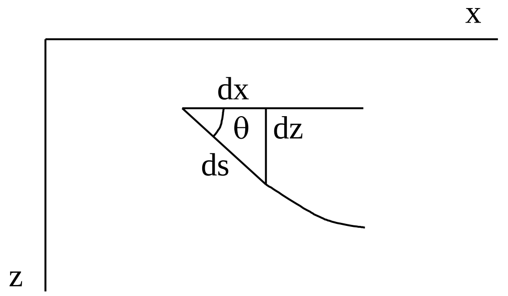


$\theta$ is grazing angle (i.e. angle relative to horizontal)

$$(1/c)(dx/ds) = \text{constant}$$

=> $$\cos\theta / c = \text{constant}$$ (Snell's Law)

Note that Snell's law for light can be written $n_1\sin\theta_1 = n_2\sin\theta_2$ where $n \propto 1/c$ and angles are angles of incidence.

or we can write

$$\frac{\cos\theta(z)}{c(z)} = \frac{\cos\theta(z_0)}{c(z_0)} \tag{2.5}$$

where $z_0$ is some reference depth usually either the source depth or the sound speed minimum.

**Calculation of ray paths**

Ray paths can be found as follows.

A ray at an angle θ to the horizontal will travel a small distance δs which will have horizontal component δr and vertical component δz.

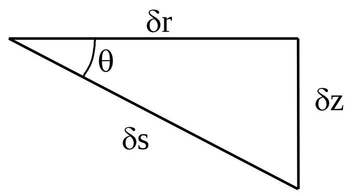


Therefore we have

$$\tan\theta = \frac{\delta z}{\delta r} \qquad \text{i.e.} \qquad \delta r = \frac{\delta z}{\tan\theta}$$

Thus at a given point a ray at angle θ moves a horizontal distance δr as it moves a vertical distance δz so we can find its new position. At the new position it has a new angle given by Snell's law.

Writing tan θ in terms of z we have

$$\tan\theta = \frac{\sin\theta}{\cos\theta} = \frac{\sqrt{1-\cos^2\theta}}{\cos\theta} = \sqrt{\frac{1}{\cos^2\theta} - 1} = \sqrt{\frac{c_s^2}{c(z)^2\cos^2\theta_s} - 1}$$

where we have taken the reference depth as the source depth $z_s$ with sound speed $c_s$ and ray angle $\theta_s$.

Combining these results we get

$$\Delta r = \left(\frac{c_s^2}{c(z)^2\cos^2\theta_s} - 1\right)^{-1/2} \Delta z \qquad \text{or} \qquad \Delta z = \left(\frac{c_s^2}{c(z)^2\cos^2\theta_s} - 1\right)^{1/2} \Delta r$$

This is the fundamental ray tracing equation. From a point (r,z) with sound speed c(z) we choose a small increment in horizontal range Δr and the new depth is z + Δz at the new range r + Δr. Repeated steps trace out the ray path for the ray which has angle $\theta_s$ at the depth where the sound speed is $c_s$. For accurate ray paths Runge-Kutta integration can be used.

The total horizontal distance travelled is given by the integral

$$r = \int_{z_s\sim}^{z} \left(\frac{c_s^2}{c(z')^2\cos^2\theta_s} - 1\right)^{-1/2} dz' \tag{2.6}$$

where the ray starts at depth $z_s$ and finishes at depth z. The notation $z_s\sim$ means that the ray path is followed as it cycles up and down.

This equation relates r and z and is the equation of the ray path for a ray launched at angle $\theta_s$.

**Cycle distance**

If the sound speed is a function of depth only, as a ray cycles up and down each complete loop is identical. The cycle distance is the horizontal distance travelled in one complete loop. If the above integral is evaluated between upper and lower turning points of the ray the result will give half the cycle distance.

Usually cycle distance changes with angle i.e. rays which cross the axis at angle $\theta_0$ will have different cycle distances for each value of $\theta_0$. If nearby rays all have the same cycle distance they will converge to a perfect focus at multiples of the cycle distance.

**Travel time**

Similarly we can find travel time.

$$\delta t = \frac{\delta s}{c} = \frac{\delta z}{c \sin \theta}$$

$$t = \int_{z_s\sim}^{z} \frac{c_s}{c(z') \sqrt{c_s^2 - c(z')^2 \cos^2\theta_s}} \, dz' \qquad (2.7)$$

**Eigenrays**

The sound field at a point due to a source at another point can be found, in principle, by summing the contributions from all possible ray paths between source and receiver. Such a ray path from source to receiver is an **eigenray**.

Eigenrays can be found numerically by tracing a ray with some starting angle until it gets to the same range as the receiver. It will usually not pass through the receiver. The starting angle is then varied until the ray passes within some acceptably small distance of the receiver.

There are usually many eigenrays. For a given number of bottom turning points there are, in general, four eigenrays. This occurs because a ray can leave the source travelling upwards or downwards and can arrive at the receiver travelling upwards or downwards giving four combinations.

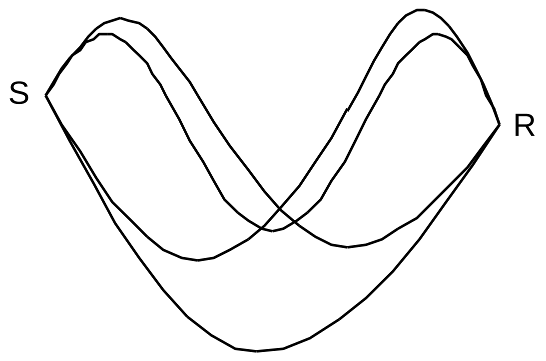


The four eigenrays with one lower turning point.

Two of the eigenrays have one upper turning point, one has zero and one has two.

In general, for the four eigenrays with n lower turning points, two will have n upper turning points, one will have n–1 and one will have n+1.

## Shadow zones

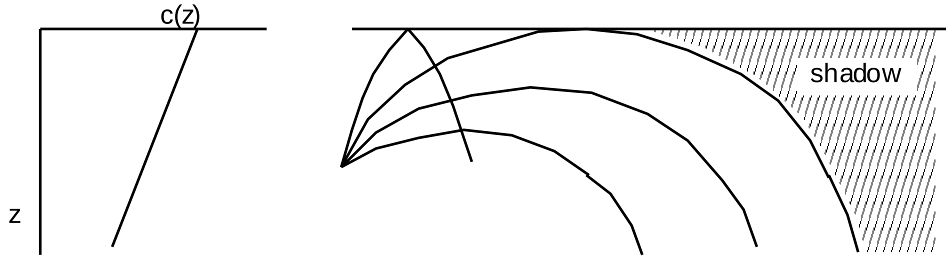


A shadow zone is a region where sound cannot reach along a ray path. In the situation shown the ray which grazes the surface forms a boundary between the insonified region and the acoustic shadow. Sharp shadows are impossible. There is always diffraction into the shadow region and ray theory must be modified to find the field in shadows.

## Focussing

Focussing of sound occurs when a number of rays pass through the same point.

## Caustics

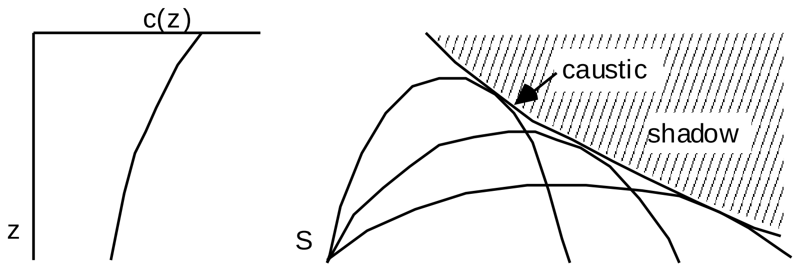


A caustic is formed when a series of rays of slightly different angles form a boundary between a shadow zone where the rays do not reach and an insonified zone where there are two rays through each point. Each ray touches the caustic in a different place.
Simple ray formulas must be modified near focusses and caustics to avoid prediction of infinite energy.

## Munk Profile

The Munk profile is an analytic expression which gives a good approximation to the variation of sound speed with depth in deep water. [Munk JASA **55**, 220-226 (1974)]

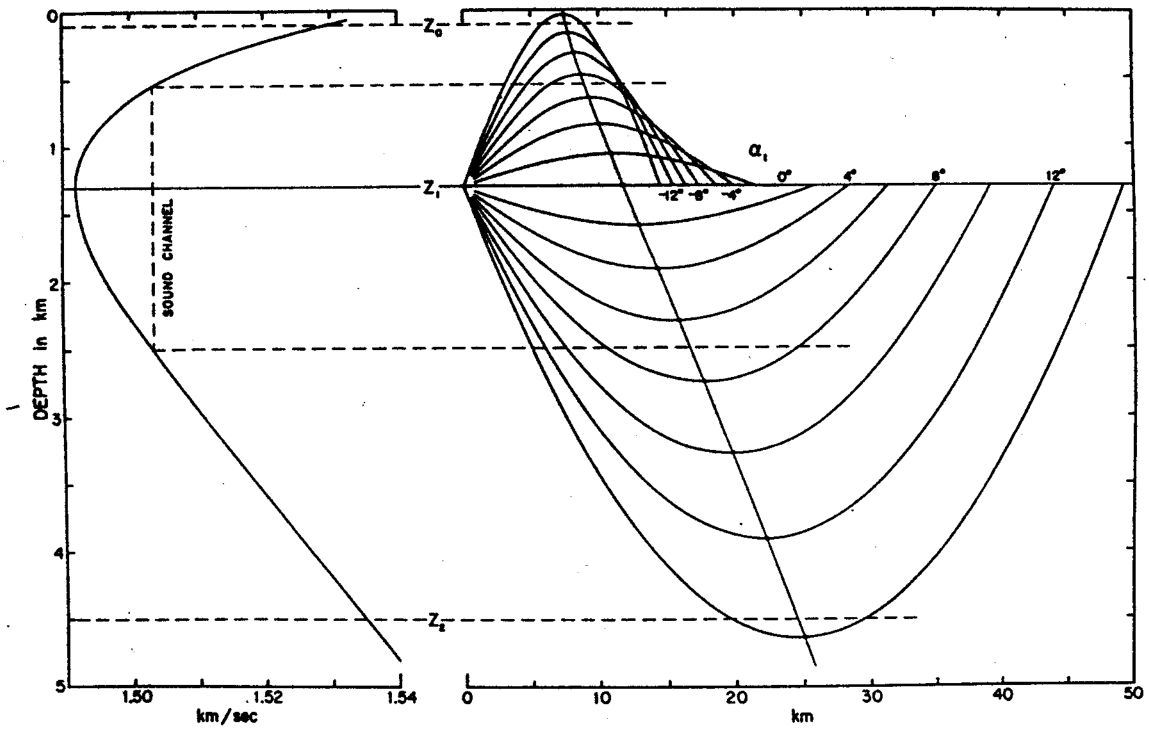


$$c(z) = c_0 \, [1 + \varepsilon(e^{-\eta} + \eta - 1)] \tag{2.8}$$

with $\eta = 2(z - z_0)/B$ and $\varepsilon = 0.0057$

The parameter $z_0$ is the depth of the sound speed minimum. The parameter B defines the 'width' of the channel. Typical values are $z_0$ = 1.3 km and B = 1.3 km.

For $z << z_0$ , approaching the surface, we have $c(z) \approx c_0 \, \varepsilon \, e^{|\eta|}$ i.e. exponential increase.

For $z >> z_0$ , approaching the bottom, we have $c(z) \approx c_0(1-\varepsilon+\varepsilon\eta)$ i.e. linear increase.

The Munk profile is very useful for studying general effects in deep water sound propagation. Notice that the change of sound speed with depth is more rapid above the minimum than it is below the minimum. This is typical of the real ocean.

The figure shows rays paths for rays at various angles emerging from a source on the axis. The following features are typical of deep water propagation.

1. The depth scale is exaggerated. Ray angles are much smaller than they look.
2. The rays are identified by their grazing angle at the axis.
3. The ray returns to the axis with the same angle as at the start.
4. The upper loops are much shorter than the lower loops.
5. There are limiting rays which just graze surface or bottom.
6. The limiting rays have quite small angles at the axis. The limiting rays typically have angles of $15^{o}$ or less.

Rays which have angles greater than the ray which just grazes the surface are reflected from the surface at an equal angle. Such rays are negligible after a few cycles because of scattering at the surface and attenuation and scattering on reflection at the bottom.

## 3. ACOUSTIC PLANE WAVES

Consider acoustic plane waves of wavelength $\lambda$

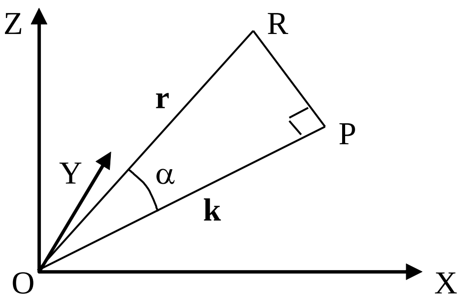


Let R be an arbitrary point on the wavefront through P. RP is perpendicular to OP.

**k** is a vector in the direction of propagation.

Take the phase at the origin as zero at time t = 0.

Phase at R (at t = 0) $=$ phase at P (at t = 0)

$$= 2\pi \times (OP / \lambda)$$

$$= (2\pi/\lambda)\, r \cos\alpha$$

$$= (2\pi/\lambda) \times (\mathbf{k.r} / k)$$

Now define wave number $k = 2\pi/\lambda$.

Phase at R (at t = 0) $= \mathbf{k.r}$

=> Phase at r $= \mathbf{k.r} - \omega t$

Pressure at R given by

$$p = p_m \exp[i(\mathbf{k.r} - \omega t)] \tag{3.1}$$

or

$$p = p_m \exp[i(k_x x + k_y y + k_z z - \omega t)]$$

The pressure must satisfy the wave equation.

Substituting

$$\left(\frac{\partial^2}{\partial x^2} + \frac{\partial^2}{\partial y^2} + \frac{\partial^2}{\partial z^2}\right) p_m \exp[i(\mathbf{k.r} - \omega t)] = \frac{1}{c^2}\frac{\partial^2}{\partial t^2}\, p_m \exp[i(\mathbf{k.r} - \omega t)]$$

$$[(ik_x)^2 + (ik_x)^2 + (ik_x)^2]\, p_m \exp[i(\mathbf{k.r} - \omega t)] = (1/c^2)\,(-i\omega)^2\, p_m \exp[i(\mathbf{k.r} - \omega t)]$$

$$k_x^2 + k_y^2 + k_z^2 = \omega^2/c^2$$

$$k^2 = \omega^2/c^2$$

$$k = \omega/c$$

Hence the phase velocity and wave number are related by

$$c = \omega/k \tag{3.2}$$

## Particle displacement and Intensity

Equation (1.3) gave

$$-\,\text{grad}\ p \;=\; \rho(\partial^2\mathbf{d}/\partial t^2)$$

$$\Rightarrow \quad -\,(\partial/\partial x, \partial/\partial y, \partial/\partial z)\, p_m \exp[i(\mathbf{k.r} - \omega t)] \;=\; \rho(\partial^2\mathbf{d}/\partial t^2)$$

$$\Rightarrow \quad -\,i\,\mathbf{k}\, p_m \exp[i(\mathbf{k.r} - \omega t)] \;=\; \rho\,(-i\omega)^2\,\mathbf{d}$$

$$\Rightarrow \quad \mathbf{d} \;=\; i\,\mathbf{k}\, p_m /(\rho\omega^2) \exp[i(\mathbf{k.r} - \omega t)] \qquad (3.3)$$

$$\text{or} \quad \mathbf{d} \;=\; \mathbf{k}\,(\rho\omega^2)^{-1}\, p_m \exp[i(\mathbf{k.r} - \omega t + \pi/2)] \qquad (3.4)$$

Equations (3.4) and (3.5) show that the displacement is in the direction of propagation i.e. sound waves are longitudinal waves. They also show that the displacement lags the pressure by a quarter of a cycle.

If A is the displacement amplitude we have

$$A \;=\; k\,(\rho\omega^2)^{-1}\, p_m$$

$$\Rightarrow \quad p_m \;=\; \rho c \omega A \qquad (3.5)$$

By considering the energy of oscillation passing through unit area per second the intensity is found to be given by

$$I \;=\; p_m^{\,2} / 2\rho c \qquad (3.6)$$

## Fluid-fluid boundary conditions

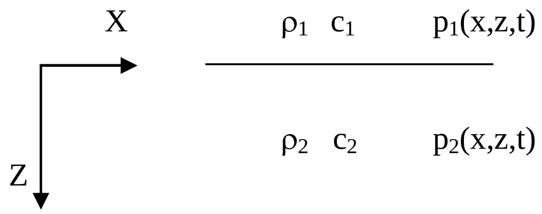


The pressure must be continuous at the boundary. Hence

$$p_1(x,0,t) \;=\; p_2(x,0,t) \qquad (3.7)$$

The displacement perpendicular to the boundary must be continuous

$$d_{1z}(x,0,t) \;=\; d_{2z}(x,0,t) \qquad (3.8)$$

Now from Eq. (1.3)

$$\text{grad}\ p \;=\; -\,\rho\,\partial^2\mathbf{d}/\partial t^2 \;=\; \rho\,\omega^2\,\mathbf{d} \qquad \text{for plane waves}$$

$$\Rightarrow \quad 1/(\rho_1\omega^2)\;(\partial p_1/\partial z) \;=\; 1/(\rho_2\omega^2)\;(\partial p_2/\partial z) \qquad \text{at boundary}$$

$$\Rightarrow \quad \frac{1}{\rho_1}\frac{\partial p_1}{\partial z} \;=\; \frac{1}{\rho_2}\frac{\partial p_2}{\partial z} \qquad \text{at boundary} \qquad (3.9)$$

## Summary of boundary conditions

Pressure continuous => $p_1 = p_2$

Displacement continuous => $\dfrac{1}{\rho_1}\dfrac{\partial p_1}{\partial z} = \dfrac{1}{\rho_2}\dfrac{\partial p_2}{\partial z}$

## ACOUSTIC PLANE WAVE REFLECTION COEFFICIENTS

### Fluid-fluid boundary

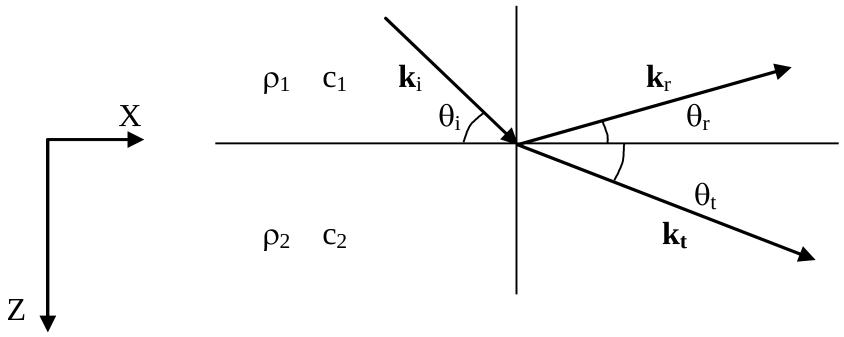


Assume an incident plane wave produces a reflected plane wave and a transmitted plane wave. Wave number vectors $\mathbf{k}_i$, $\mathbf{k}_r$ and $\mathbf{k}_t$ as shown. Note that we have not assumed $\theta_r = \theta_i$.

$$\mathbf{k}_i = (k_1\cos\theta_i, 0, k_1\sin\theta_i) \qquad \mathbf{k}_r = (k_1,\cos\theta_r, 0, -k_1\sin\theta_r) \qquad \mathbf{k}_t = (k_2\cos\theta_t, 0, k_2\sin\theta_t)$$

Field in medium 1

$$p_1 = p_i \exp[i(k_1\cos\theta_i x + k_1\sin\theta_i z - \omega t)] + p_r \exp[i(k_1\cos\theta_r x - k_1\sin\theta_r z - \omega t)] \qquad (3.10)$$

Field in medium 2

$$p_2 = p_t \exp[i(k_2\cos\theta_t x + k_2\sin\theta_t z - \omega t)] \qquad (3.11)$$

Now apply boundary conditions.

Requiring continuity of pressure at $z = 0$, the time dependence cancels out and we obtain

$$p_i \exp[i(k_1\cos\theta_i x)] + p_r \exp[i(k_1\cos\theta_r x)] = p_t \exp[i(k_2\cos\theta_t x)] \qquad (3.12)$$

This must be true for all x, hence x must cancel out. Thus we require

$$k_1\cos\theta_i = k_1\cos\theta_r = k_2\cos\theta_t \qquad (3.13)$$

Hence

$$\theta_i = \theta_r \qquad \text{Law of Reflection} \qquad (3.14)$$

and since $k = \omega/c$

$$\frac{\cos\theta_i}{c_1} = \frac{\cos\theta_t}{c_2} \qquad \text{Snell's Law} \qquad (3.15)$$

Substituting (3.13) in (3.12) gives

$$p_i + p_r = p_t \qquad (3.16)$$

Continuity of displacement requires

$$\frac{1}{\rho_1}\frac{\partial p_1}{\partial z} = \frac{1}{\rho_2}\frac{\partial p_2}{\partial z} \qquad (3.17)$$

at z = 0. Inserting $p_1$ and $p_2$ from (3.10) and (3.11) into (3.17) the x and t dependence cancel out giving

$$(1/\rho_1)\,[p_i k_1 \sin\theta_i - p_r k_1 \sin\theta_r] = (1/\rho_2)\, p_t k_2 \sin\theta_t$$

Putting $k = \omega/c$ $\theta_i = \theta_r = \theta_1$ $\theta_t = \theta_2$

gives

$$(p_i - p_r)\,\rho_2 c_2 \sin\theta_1 = p_t\,\rho_1 c_1 \sin\theta_2 \qquad (3.18)$$

**Reflection coefficient** R

Define

$$R = p_r / p_i$$

Eliminating $p_t$ from (3.16) and (3.18) gives

$$R = \frac{\rho_2 c_2 \sin\theta_1 - \rho_1 c_1 \sin\theta_2}{\rho_2 c_2 \sin\theta_1 + \rho_1 c_1 \sin\theta_2} \qquad (3.19)$$

**Transmission coefficient** T

Define

$$T = p_t / p_i$$

Eliminating $p_r$ from (3.16) and (3.18) gives

$$T = \frac{2\rho_2 c_2 \sin\theta_1}{\rho_2 c_2 \sin\theta_1 + \rho_1 c_1 \sin\theta_2} \qquad (3.20)$$

1. For normal incidence $\theta_1 = 90^o$, $\theta_2 = 90^o$

   $$R = (\rho_2 c_2 - \rho_1 c_1)/(\rho_2 c_2 + \rho_1 c_1)$$

   Hence no reflection if $\rho_2 c_2 = \rho_1 c_1$

2. Acoustic impedance defined as ratio of pressure to particle velocity for plane waves and is $\rho c$ for the material. Matching impedances gives no reflection.

3. $R > 0$ for $\rho_2 c_2 > \rho_1 c_1$ no phase reversal for reflection from higher impedance

   $R < 0$ for $\rho_2 c_2 < \rho_1 c_1$ phase reversal for reflection from lower impedance

   $T > 0$ no phase change for transmitted wave

4. $\theta_1 \to 0^o \Rightarrow R \to -1$ always total reflection at grazing incidence

5. R, T conserve energy

6. Water-air interface

| | | | |
|---|---|---|---|
| water | $\rho = 1000$ kg/m$^3$ | $c = 1500$ m/s | $\rho c = 1.5 \times 10^6$ kg/m$^2$s |
| air | $\rho = 1.3$ kg/m$^3$ | $c = 340$ m/s | $\rho c = 440$ kg/m$^2$s |

Hence

for water –> air $\quad \rho_2 \to 0 \quad R \to -1 \quad$ total reflection, phase reversal

for air –> water $\quad \rho_1 \to 0 \quad R \to 1 \quad$ total reflection, no phase reversal

**Critical Angle**

The angle $\theta_2$ is given by Snell's Law $\quad \cos\theta_2 = (c_2/c_1)\cos\theta_1$.

For $c_2 > c_1$ we have $\theta_2 < \theta_1$ giving $\theta_2 = 0^o$ for $\theta_1 = \theta_c$ the critical angle.

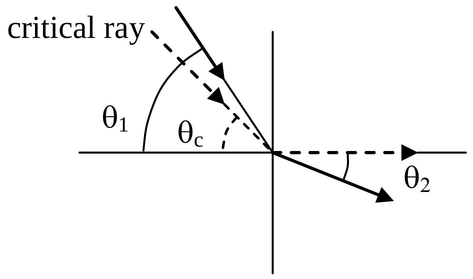


The critical angle $\theta_c$ is the value of $\theta_1$ for which $\theta_2 = 0$ and is given by

$$\cos\theta_1 = c_1/c_2$$

**Total Internal Reflection**

If the grazing angle is less than the critical angle i.e $\theta_1 < \theta_c$ we can use

$$\begin{aligned}\sin\theta_2 &= (1 - \cos^2\theta_2)^{1/2} \\ &= \left(1 - [(c_2/c_1)\cos\theta_1]^2\right)^{1/2} \\ &= i\left([(c_2/c_1)\cos\theta_1]^2 - 1\right)^{1/2}\end{aligned}$$

$$\Rightarrow \quad R = \frac{\rho_2 c_2 \sin\theta_1 - \rho_1 c_1 \; i\left([(c_2/c_1)\cos\theta_1]^2 - 1\right)^{1/2}}{\rho_2 c_2 \sin\theta_1 + \rho_1 c_1 \; i\left([(c_2/c_1)\cos\theta_1]^2 - 1\right)^{1/2}} \qquad (3.21)$$

$$\Rightarrow \quad R = |R| \exp[i\phi]$$

where $|R| = 1$ $\quad$ i.e. total reflection

$$\text{and} \quad \phi = -2\tan^{-1}\left(\frac{\rho_1 c_1 \left([(c_2/c_1)\cos\theta_1]^2 - 1\right)^{1/2}}{\rho_2 c_2 \sin\theta_1}\right) \qquad (3.22)$$

Hence $\phi = 0$ $\quad$ for $\theta_1 = \theta_c$

and $\phi \to -\pi$ $\quad$ for $\theta_1 \to 0^o$

Therefore for $\theta_1 < \theta_c$ there is total reflection with an angle dependent phase change.

**Field in medium 2 for total internal reflection**

$$p_2 = T\, p_i \exp[i(k_2\cos\theta_t x + k_2\sin\theta_t z - \omega t)]$$

$$= \frac{2\rho_2 c_2 \sin\theta_1}{\rho_2 c_2 \sin\theta_1 + i\rho_1 c_1\left([(c_2/c_1)\cos\theta_1]^2 - 1\right)^{1/2}}\; p_i \exp[i(k_1\cos\theta_1 x - \omega t)] \exp[-k_2\left([(c_2/c_1)\cos\theta_1]^2 - 1\right)^{1/2} z] \qquad (3.23)$$

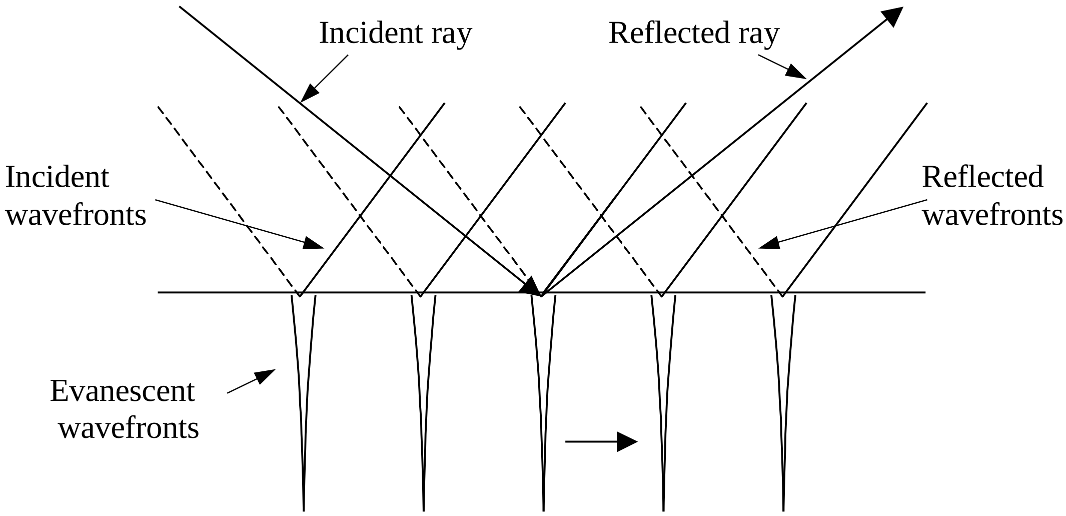


The field in medium 2 travels parallel to the boundary with wavefronts perpendicular to the boundary. There is exponential decay of amplitude away from the boundary. Such waves are called **evanescent waves** or **inhomogeneous waves** and satisfy the wave equation.

## 4. NORMAL MODE PROPAGATION

### Standard problem

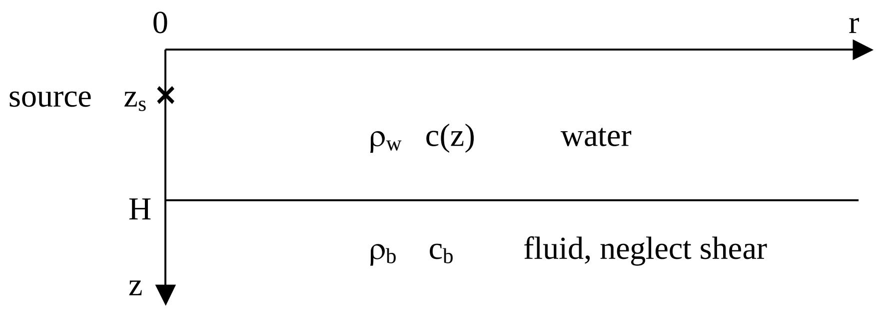


### Wave Equation

The wave equation in cylindrical coordinates for a harmonic source of angular frequency ω can be written

$$\frac{\partial^2 p}{\partial r^2} + \frac{1}{r}\frac{\partial p}{\partial r} + \frac{\partial^2 p}{\partial z^2} + \frac{\omega^2}{c^2}\, p = 0 \qquad (4.1)$$

The normal mode solution to the wave equation is referred to as a **full wave solution** because it solves the wave equation exactly. However, the solution is restricted to horizontally stratified situations i.e. there is no range dependence such as a sloping bottom.
The main feature of normal mode solutions is that the wave equation is assumed to be separable. i.e. it is assumed that the solution for p(r,z) can be written as a product of functions of r and z as

$$p(r,z) = R(r)\, Z(z) \qquad (4.2)$$

this then enables the wave equation to be separated into an equation for R(r) and an equation for Z(z).
The equations are

$$\frac{d^2R}{dr^2} + \frac{1}{r}\frac{dR}{dr} + k^2 R = 0 \qquad (4.3)$$

$$\frac{d^2Z}{dz^2} + \frac{\omega^2}{c(z)^2} Z - k^2 Z = 0 \qquad (4.4)$$

Note that this separation is only possible because the sound speed c is a function of depth only.

The parameter k is a separation constant and corresponds physically to the **horizontal wave number**.

### Radial solution

The solution for R is the Hankel function $H_0^{(1)}(kr)$ which is just a power series in kr. It has the convenient asymptotic form

$$H_0^{(1)}(kr) \sim (2/\pi kr)^{1/2} \exp[i(kr - \pi/4)] \qquad (4.5)$$

The asymptotic form is very accurate except within one wavelength of the source and is used in most applications.
The amplitude depends on range as $r^{-1/2}$ which is consistent with energy conservation for cylindrical spreading. With assumed time dependence $\exp(-i\omega t)$ the phase dependence $\exp(ikr-\omega t)$ represents a wave travelling in the radial direction with wave number k. Thus Eq. (4.5) represents a **cylindrical wave** propagating outward from the origin.

## Depth solution

$$\frac{d^2Z}{dz^2} + \left[ \frac{\omega^2}{c(z)^2} - k^2 \right] Z = 0 \qquad (4.6)$$

The function Z(z) oscillates while the term in square brackets is positive.
[ The equation resembles $d^2Z/dz^2 + a^2 Z = 0$ which has solution $Z = A \sin az$ ]
The function decays (or grows) exponentially when the term in square brackets is negative.
[ The equation resembles $d^2Z/dz^2 - a^2 Z = 0$ which has solution $Z = A e^{\pm az}$ ]

The solution of the depth equation depends on the precise form of the sound speed profile c(z).
It is convenient to define $c_0$ as the lowest value of sound speed in the water.

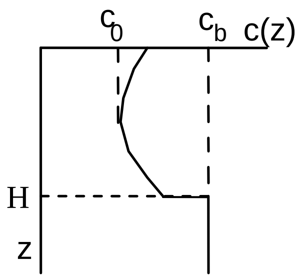


With the boundary conditions at z = H the depth solutions are of three types

(i) **Discrete modes**
There are a finite number of solutions with
$\omega/c_b < k < \omega/c_0$
The energy in these solutions is confined to the water layer. These solutions are sometimes referred to as the **trapped modes**. The energy propagates to great ranges and the signals received at medium to large ranges are due entirely to the discrete modes.

(ii) **Continuous modes**
The equation has solutions for any k value when
$0 < k < \omega/c_b$
These solutions oscillate everywhere and represent energy which leaks into the bottom. They only contribute to the sound field at short ranges and are ignored in most applications.

(iii) **Evanescent modes**
The equation has solutions for any k when
$k^2 < 0$
the value of k is pure imaginary and solutions decay rapidly with range. They are ignored in most applications.

We will first consider a simple shallow water situation as this contains most of the features of the general case without too many complications.

## Pekeris model

The Pekeris model provides a good approximation to the shallow water situation.

The model consists of a homogeneous fluid of depth H over a homogeneous fluid half space and provides the simplest realistic model for shallow water acoustics.

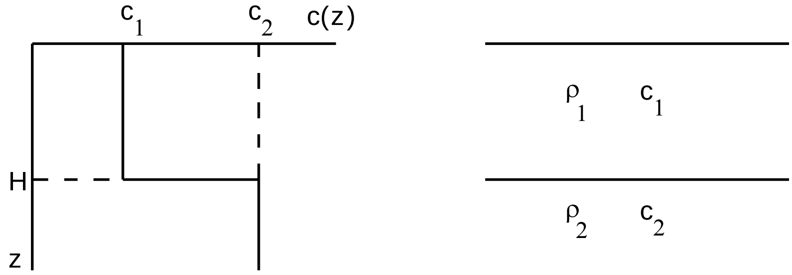


The depth separated equation

$$\frac{d^2Z}{dz^2} + \left( \frac{\omega^2}{c(z)^2} - k^2 \right) Z = 0 \qquad (4.7)$$

has solution

$$Z(z) = A \sin \gamma z \qquad z < H \qquad (4.8)$$

$$\gamma^2 = \frac{\omega^2}{c_1{}^2} - k^2 \qquad (4.9)$$

$$Z(z) = B \exp[-\nu z] \qquad z > H \qquad (4.10)$$

$$\nu^2 = k^2 - \frac{\omega^2}{c_2{}^2} \qquad (4.11)$$

## Boundary conditions

Our solution must satisfy the physical boundary conditions as follows.

1. The pressure must vanish at the surface because the reflection coefficient at the surface is –1. Hence we require

   $$p(r,0) = 0 \quad \text{i.e.} \quad Z(0) = 0 \qquad (4.12)$$

   We have already used this boundary condition in choosing the sine function rather than cosine.

2. The pressure must approach zero at great depth otherwise there would be infinite energy. Hence we require

   $$p(r,z) \to 0 \quad \text{i.e.} \quad Z(z) \to 0 \text{ as } z \to \infty \qquad (4.13)$$

   We have already used this boundary condition in choosing the decaying exponential in (4.10).

3. The pressures must be equal on both sides of the interface.

   $$p(r,H^+) = p(r,H^-) \quad \text{i.e.} \quad Z(H^+) = Z(H^-) \qquad (4.14)$$

4. The z-component of particle displacements must be equal on both sides of the interface. Since particle displacement is proportional to $\frac{1}{\rho}\left(\frac{\partial p}{\partial z}\right)$

   we require

   $$Z'(H^+)/\rho_1 = Z'(H^-)/\rho_2 \qquad (4.15)$$

   where Z' means dZ/dz

Algebra leads to

$$\tan\left(\sqrt{\frac{\omega^2}{c_1^2} - k^2}\, H\right) = -\frac{\rho_2}{\rho_1}\frac{\sqrt{\frac{\omega^2}{c_1^2} - k^2}}{\sqrt{k^2 - \frac{\omega^2}{c_2^2}}} \tag{4.16}$$

This is an eigenvalue equation in k. The discrete values of k which satisfy this equation are called the normal mode eigenvalues $k_n$ where the subscript identifies mode n. In this simple application the eigenvalues are obtained from a transcendental equation. In real world problems the eigenvalues are obtained by numerical solution of the depth equation (4.7).

Discrete solutions exist only for

$$\frac{\omega}{c_1} > k > \frac{\omega}{c_2}$$

or in terms of phase velocity $\omega/k$, solutions exist only for

$$c_1 < \frac{\omega}{k} < c_2$$

i.e. the normal mode solutions have a phase velocity which lies between the velocity in the water and the velocity in the bottom.

In the present example it is easier to work in terms of $\gamma$ and to solve

$$\tan \gamma H = -\frac{\rho_2}{\rho_1}\frac{\gamma}{\sqrt{\frac{\omega^2}{c_1^2} - \frac{\omega^2}{c_2^2} - \gamma^2}} \tag{4.17}$$

The equation must be solved numerically. A graphical solution can be found by drawing a graph of both sides and noting the points of intersection.

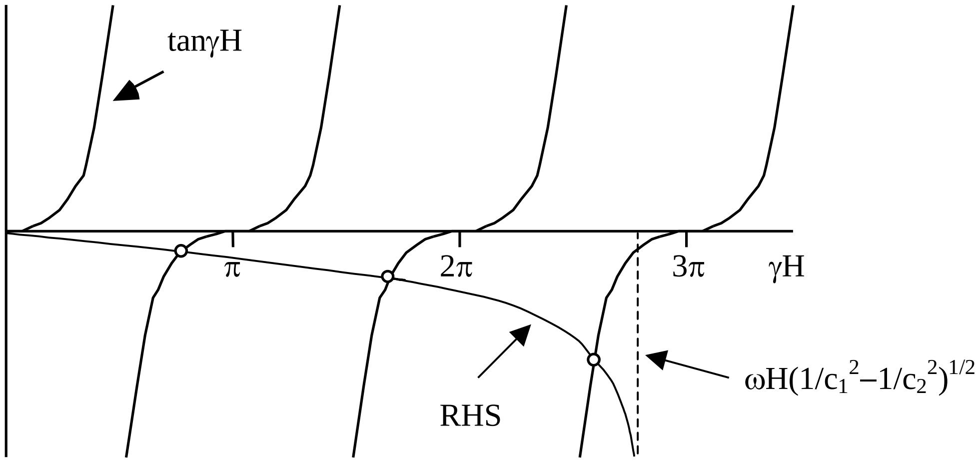


Notice that the number of solutions increases as $\omega$ or H increases.

If the values for $\gamma$ are labelled $\gamma_n$ the normal modes are

$$U_n(z) = A_n \sin \gamma_n z \qquad z < H \tag{4.18}$$

$$= A_n \sin \gamma_n H \ \exp[\nu_n (H - z)] \qquad z > H \qquad (4.19)$$

It is convenient to normalise the normal modes so that

$$\int_0^\infty (U_n^2 / \rho)\, dz = 1$$

giving

$$A_n = \left[ \frac{1}{\rho_1} \left( \frac{H}{2} - \frac{\sin 2\gamma_n H}{4\gamma_n} \right) + \frac{1}{\rho_2} \frac{\sin^2 \gamma_n H}{2\nu_n} \right]^{-1/2} \qquad (4.20)$$

Example.

| | | |
|---|---|---|
| $H = 50$ m | $c_1 = 1500$ m/s | $c_2 = 1610$ m/s |
| $\rho_1 = 1$g/cc | $\rho_2 = 1.5$ g/cc | $f = 120$ Hz |

| Mode No. | Eigenvalues | | | |
|---|---|---|---|---|
| n | $k_n$ | $\gamma_n$ | $\nu_n$ | $\omega/k_n$ |
| 1 | 0.499733 | 0.054119 | 0.174404 | 1508.77 |
| 2 | 0.490721 | 0.108878 | 0.146599 | 1536.48 |
| 3 | 0.475325 | 0.163486 | 0.081352 | 1586.25 |

The mode functions can be plotted as follows.

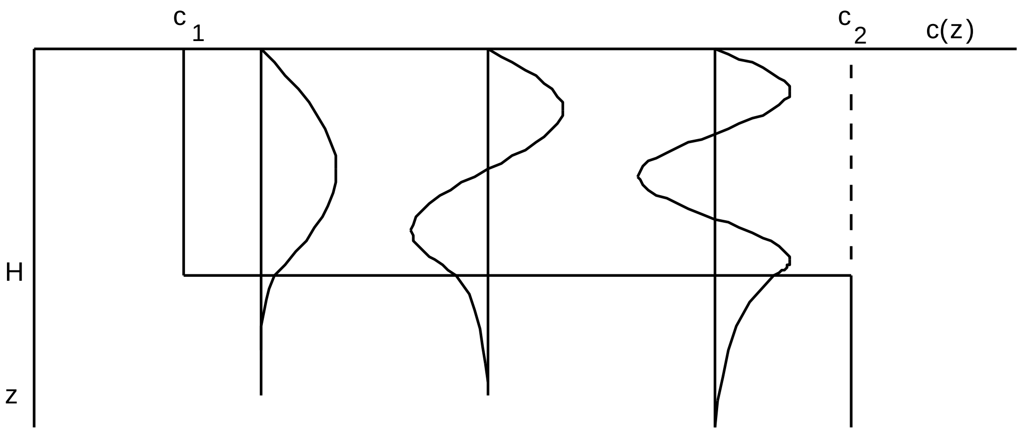


It is conventional to plot each normal mode superimposed on the velocity profile at its phase velocity $\omega/k_n$.

Notice that the n-th normal mode has n maxima as depth changes. The normal modes oscillate in the water and decay exponentially in the bottom.

**Normal modes**

The normal mode functions $U_n(z)$ are constructed from the solutions for Z(z).

They have the properties

(i) $$\int_0^\infty (U_n^2/\rho)\, dz = 1 \qquad (4.21)$$

(ii) $$\int_0^\infty (U_n U_m/\rho)\, dz = 0 \qquad n \neq m \qquad (4.22)$$

Therefore the normal modes are orthogonal with weight function $1/\rho(z)$ where $\rho(z)$ is the constant density in each layer. Equation (4.21) leads to

$$U_n(z) = N_n Z_n(z) \qquad (4.23)$$

$$N_n = \left[ \int_0^\infty \frac{Z_n^2(z)}{\rho(z)}\, dz \right]^{-1/2} \qquad (4.24)$$

**General solution**

The solution for a point harmonic source of angular frequency $\omega$ at $r = 0$, $z = z_s$ is

$$p(r,z) = i\,\pi\, [Q/\rho(z_s)] \sum_1^N U_n(z_s)\, U_n(z)\, H_0^{(1)}(k_n r) \qquad (4.25)$$

The explicit derivation of this expansion can be obtained from a transform solution of the wave equation.

Using the asymptotic form of the Hankel function the pressure is given by

$$p(r,z) = [2\pi/r]^{1/2}\, [Q/\rho(z_s)]\, e^{i\pi/4} \sum_1^N U_n(z_s)\, U_n(z)\;\; k_n^{-1/2} \exp(ik_n r) \qquad (4.26)$$

Notice that each term of the solution is a product of a function of r and a function of z as was assumed during separation of variables.

The amount of each normal mode present is proportional to $U_n(z_s)$ i.e. the magnitude of the normal mode at the depth of the source. This corresponds to physical intuition in that if the source is on the maximum of a mode it will strongly excite that mode. Conversely, if the source is on the null of a mode then that mode will not be excited at all.

**Normal Mode Tank Experiment** (Tindle et al. J. Acoust. Soc. Am. 81 275-286 (1987))

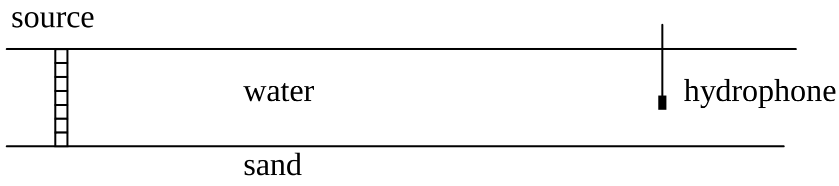


The experimental arrangement had a layer of water 10 cm deep and sound speed 1490 m/s over a sand bottom of sound speed 1784 m/s. The density ratio was 1.97.

The source was a vertical stack with 7 elements that could generate single modes by matching the phase and amplitude of the mode at the corresponding depth. The source waveform measurements were made near the source array with elements excited one at a time. The sources transmit a smoothed 4 cycle pulse at 80 kHz.

The receiver was a small hydrophone which could be moved continuously as a function of depth.

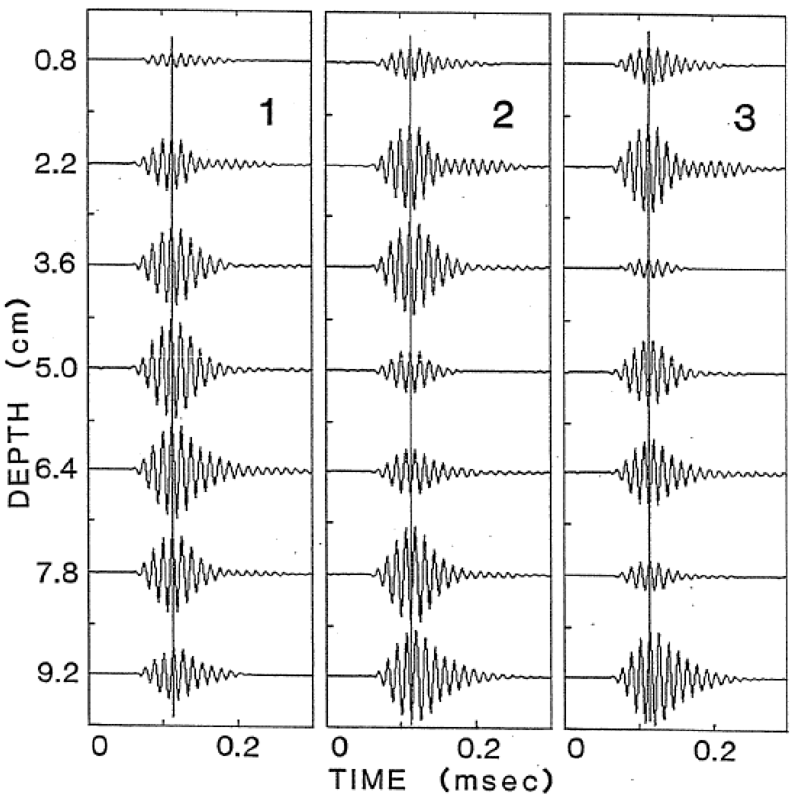


Figure 1 shows the source waveforms at the source element depths for the first three modes.
The vertical lines and the peaks in the waveforms show that for mode 1 all sources are in phase. For mode 2 the upper four sources are in phase and the lower three are phase reversed. For mode three the upper three sources are in phase, the next two are phase reversed and the lower two are in phase with the upper three.

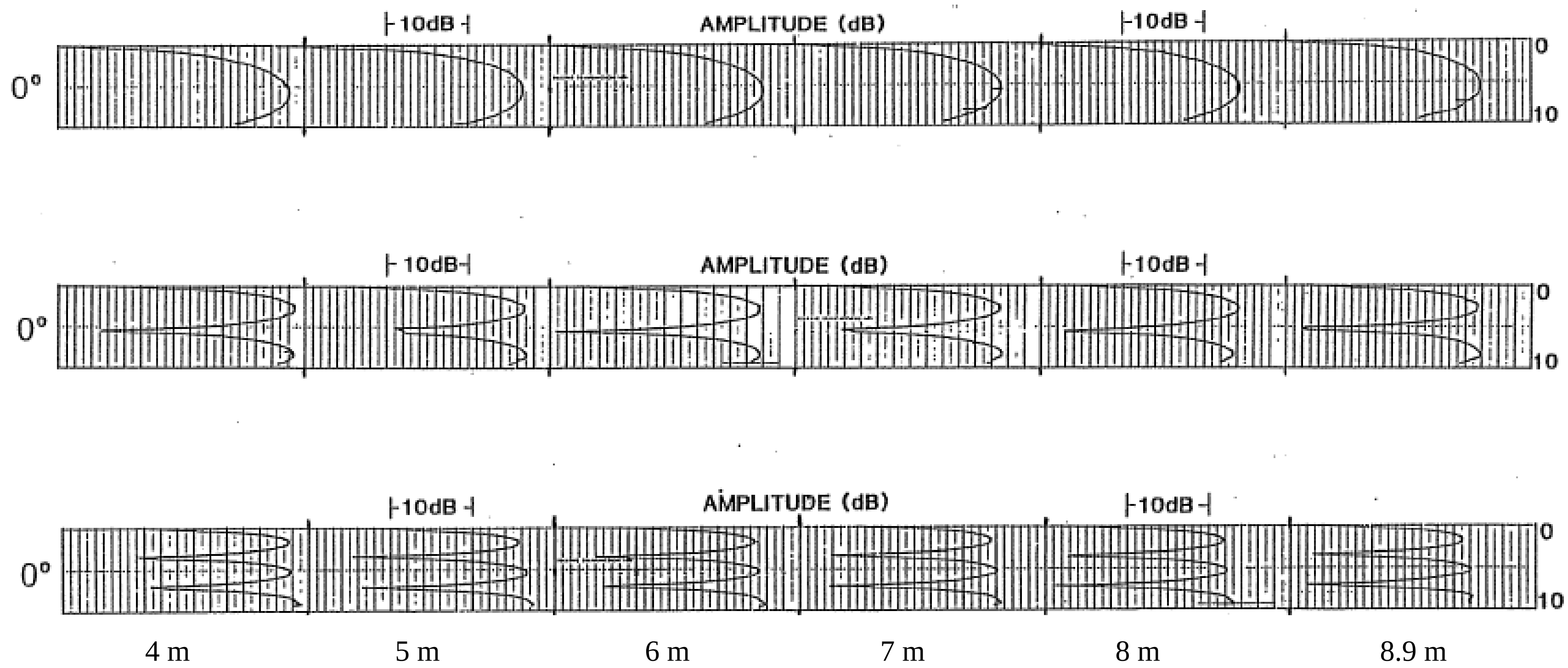


Figure 2 shows the shape (on a dB scale) of each mode as a function of depth at successive ranges.
The amplitude is the peak level of the pulse at the given depth.

Each mode retains its amplitude as a function of depth as it propagates in range.

Each mode slowly loses amplitude as a function of range and the rate of attenuation increases with mode number.

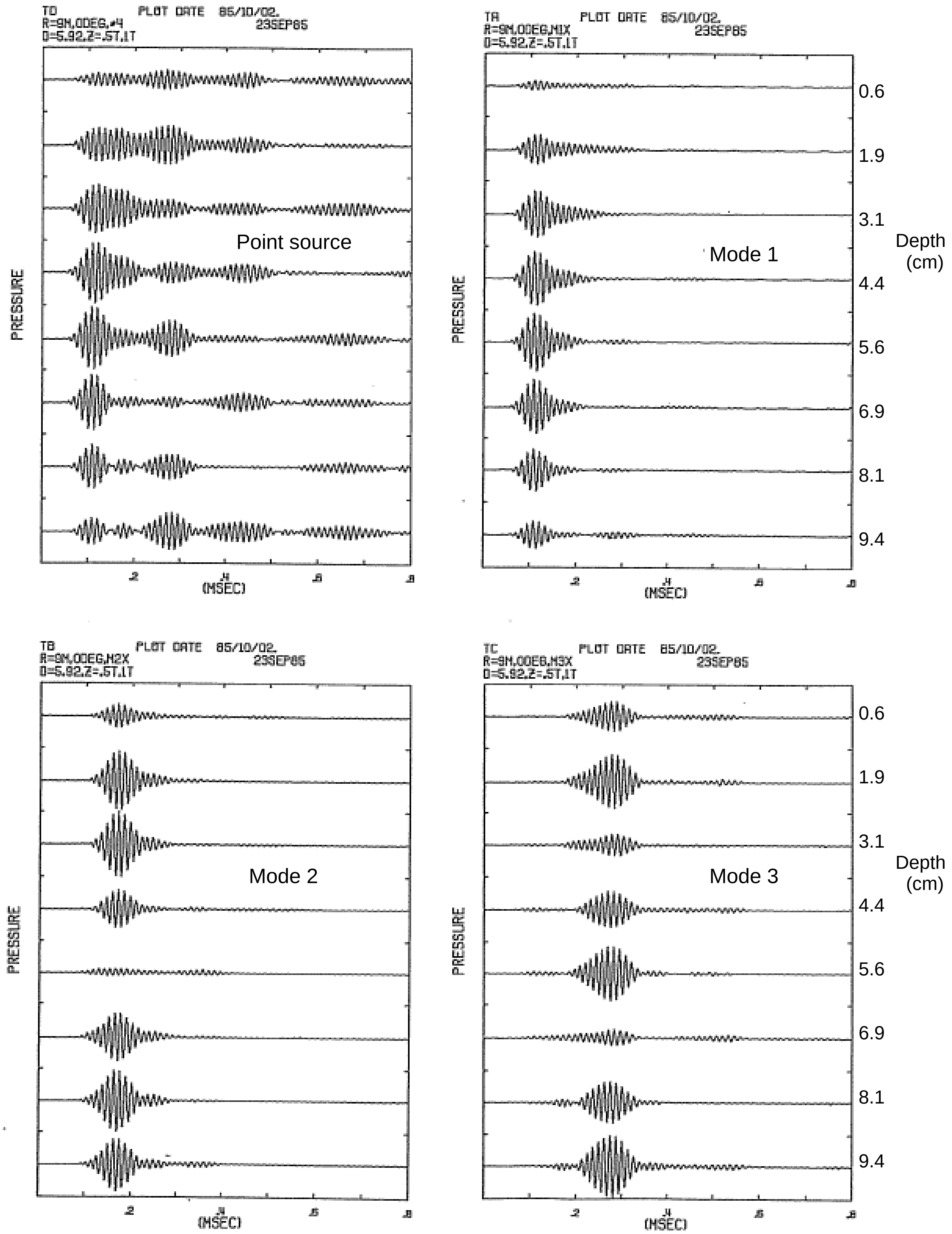


Figure 3 shows waveforms recorded at 8 evenly spaced depths at a range of 8.9m.
The upper left figure is for a point source (the 4th element of the array). Each mode is excited with an amplitude proportional to its amplitude at the depth of the source element.
The waveforms show five successive arrivals corresponding to the first five modes. The amplitude of mode two is fairly small because the source is near a null of mode two.
Successive pulses are increased in length compared to the source pulses because of dispersion.
The other figures show the waveforms obtained when the source array transmits a single mode. Each mode arrives at a different time corresponding to the time in the upper left figure. Each mode has the amplitude and phase dependence as a function of depth characteristic of that mode.

## Attenuation

The replacement $\omega/c \to \omega/c + i\alpha$ can be used in normal mode theory to include the effects of attenuation.
Since attenuation is usually small we can assume $\alpha << \omega/c$ and use perturbation theory.

We assume the normal modes and eigenvalues are changed slightly

i.e. $U_n(z) \to U_n(z) + \Delta U_n(z)$ and $k_n \to k_n + \Delta k_n$

The normal modes satisfy

$$U_n'' + (\omega^2/c^2 - k_n^2)\, U_n = 0 \tag{4.27}$$

where the primes indicate d/dz. Substitution gives

$$U_n'' + (\Delta U_n)'' + [(\omega/c + i\alpha)^2 - (k_n + \Delta k_n)^2]\,(U_n + \Delta U_n) = 0 \tag{4.28}$$

Expanding, substituting for $U_n''$ from Eq. (4.27) and keeping only first order terms leads to

$$(\Delta U_n)'' + (\omega^2/c^2 - k_n^2)\,\Delta U_n + (2i\alpha\omega/c - 2k_n\Delta k_n)\, U_n = 0 \tag{4.29}$$

Now let

$$\Delta U_n(z) = \sum_m a_m U_m(z) \tag{4.30}$$

This is possible because the $U_n$ form a complete set.
Differentiating we have

$$(\Delta U_n)'' = \sum_m a_m U_m''$$

and substituting using Eq. (4.27) gives

$$(\Delta U_m)'' = -\sum_m a_m (\omega^2/c^2 - k_m^2)\, U_m \tag{4.31}$$

Substitution of Eqs. (4.30) and (4.31) into (4.29) gives

$$-\sum_m a_m (\omega^2/c^2 - k_m^2)\, U_m + (\omega^2/c^2 - k_n^2) \sum_m a_m U_m + (2i\alpha\omega/c - 2k_n\Delta k_n)\, U_n = 0$$

The terms in $\omega^2/c^2$ cancel giving

$$\sum_m a_m (k_m^2 - k_n^2)\, U_m + (2i\alpha\omega/c - 2k_n\Delta k_n)\, U_n = 0$$

Multiplying by $U_n/\rho$ and integrating $(0,\infty)$ allows us to use mode orthogonality as in Eq. (4.22) and mode normalisation as in Eq. (4.21) to obtain

$$\Delta k_n = \frac{i\omega}{k_n}\int_0^\infty \frac{\alpha(z)}{\rho(z)c(z)} U_n^2(z)\, dz \qquad (4.32)$$

Since $\Delta k_n$ is pure imaginary we set $\Delta k_n = i\delta_n$ to obtain

$$\delta_n = \frac{\omega}{k_n}\int_0^\infty \frac{\alpha(z)}{\rho(z)c(z)} U_n^2(z)\, dz \qquad (4.33)$$

The term $\exp(ik_n r)$ in the mode sum becomes $\exp(ik_n r)\exp(-\delta_n r)$ so that each mode is attenuated at its own rate.

For shallow water modes the attenuation in the bottom dominates.

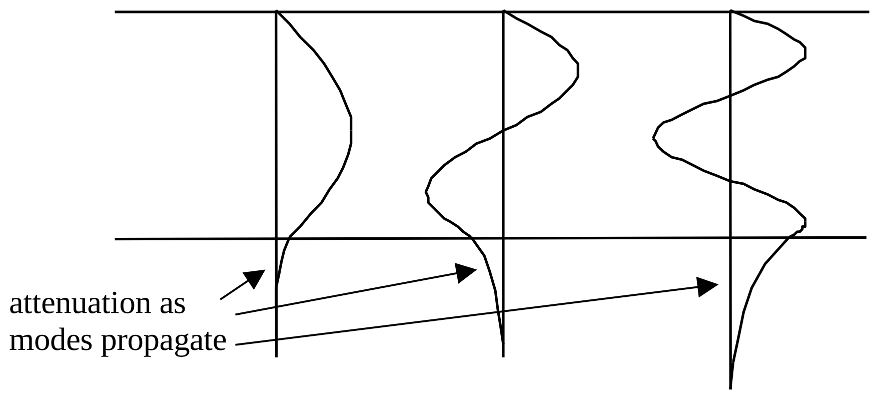


Mode amplitude decays with range as the bottom absorbs energy. Usually higher modes decay more rapidly.

For the case of the Pekeris two fluid model as given above the attenuation is zero in the water so the integration is over the range $(H,\infty)$ and the sound speed $c_2$ is constant. The result is

$$\delta_n = \frac{\omega\alpha}{c_2 k_n}\,\frac{\rho_1\rho_2\gamma_n^2}{\nu_n H[(\rho_2\gamma_n)^2 + (\rho_1\nu_n)^2] + \rho_1\rho_2(\gamma_n^2 + \nu_n^2)} \qquad (4.34)$$

## 5. NORMAL MODES AND BROADBAND PROPAGATION

For time dependent signals the source will have a frequency spectrum $S(\omega)$ and the full time dependent solution becomes

$$p(r,z,t) = i\,\pi\,[Q/\rho(z_s)] \int S(\omega) \sum_{1}^{N} U_n(z_s)\,U_n(z)\;\; H_0^{(1)}(k_n r)\;\; e^{-i\omega t}\, d\omega \qquad (5.1)$$

Note that the summation over modes needs to be inside the integral over frequency because the number N of discrete modes is a function of frequency.

Inserting the asymptotic form of the Hankel function gives

$$p(r,z,t) = [2\pi/r]^{1/2}\,[Q/\rho(z_s)]\, e^{i\pi/4} \int S(\omega) \sum_{1}^{N} U_n(z_s)\,U_n(z)\;\; k_n^{-1/2} \exp[i(k_n r - \omega t)]\, d\omega \qquad (5.2)$$

## Wave packets and dispersion

Consider an acoustic field given by

$$p = p_0 \exp[i(kx - \omega t)] \qquad (5.3)$$

This represents a succession of infinite plane waves travelling in the X direction with no start and no finish.

Points of constant phase travel with **phase velocity** v given by

$$v = \omega/k.$$

A pulse or wave packet may be constructed by combining waves of different frequencies

$$p(x,t) = \int_{-\infty}^{\infty} G(\omega) \exp[i(kx - \omega t)]\, d\omega \qquad (5.4)$$

If $G(\omega)$ is non zero only near $\omega_0$ then only values near $\omega_0$ contribute to the integral.

Let

$$\phi(x,t,\omega) = kx - \omega t \qquad (5.5)$$

giving

$$p(x,t) = \int_{-\infty}^{\infty} G(\omega) \exp(i\phi) d\omega \qquad (5.6)$$

If $\phi$ varies rapidly for some x,t value then p –> 0 because the integrand oscillates rapidly. Hence p is localised to regions where $\phi$ is slowly varying i.e. $\partial\phi/\partial\omega$ is small or zero.

Putting

$$\partial\phi/\partial\omega \,\Big|_{\omega_0} = 0$$

$$\Rightarrow \quad [dk/d\omega \,\big|_{\omega_0}]\, x - t = 0.$$

We deduce that $p(x,t) \approx 0$ unless

$$x/t \approx d\omega/dk \,\Big|_{\omega_0}$$

Hence the pulse or group moves at the **group velocity** u given by

$$u = d\omega/dk \qquad (5.7)$$

If $k(\omega) = \omega/c$ with c constant we have

$$p(x,t) = \int_{-\infty}^{\infty} G(\omega) \exp[i(\omega/c)(x - ct)]\, d\omega$$

which is constant for a given value of x–ct i.e. the pulse travels undistorted at speed c.

For other $k(\omega)$ the pulse changes shape as it travels and there is pulse spreading or dispersion.

**Material dispersion** (also called intrinsic dispersion)

This occurs if the propagation speed of a plane wave is a function of frequency e.g. optics.
There is no material dispersion in acoustics or seismics.

## Geometric dispersion

Waveguides give rise to geometric dispersion because the component of the propagation vector along the waveguide is a function of frequency. Thus a pulse travelling along the waveguide will change shape as it travels.

**Pekeris model dispersion curves**

The phase velocity $v_n = \omega/k_n$ and group velocity $u_n = d\omega/dk_n$ can be plotted as a function of ω to give the dispersion curves.

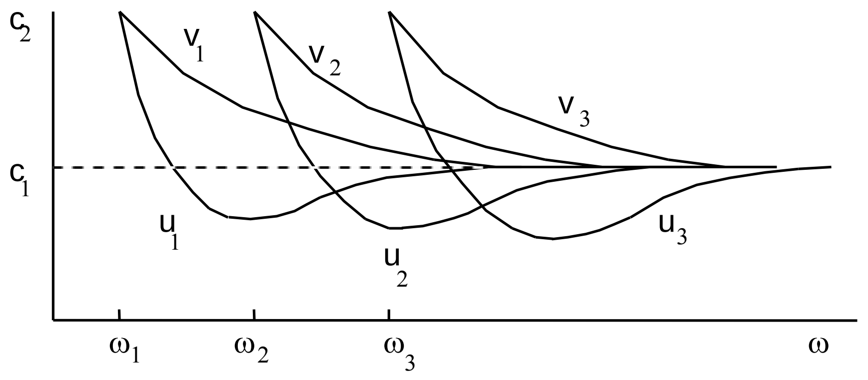


The group velocity curves provide the main physical interest because pulses travel at the group velocity.

The group velocity curves can be used to anticipate the structure of a received signal.

- Each mode has a lower cutoff frequency below which it does not propagate.
- If a transmitted signal contains all frequencies the lowest frequency in each mode arrives first because it has group velocity $c_2$.

  Then the frequency in each mode rises steadily until the components at velocity $c_1$ arrive.

  Next there are both high and low frequency components in each mode, with the frequency of the high frequency components dropping rapidly.
- Each group velocity curve has a minimum. Hence for each mode there is a frequency which travels slowest and arrives last.

**Calculation of group velocity**

It is difficult to find $d\omega/dk_n$ analytically, except in trivial problems, and it is impossible if the velocity profile, c(z), is given by a set of numerical values.

It is easier to find the group velocity from the finite differential ratio $\Delta\omega/\Delta k_n$ by finding the eigenvalues at two nearby values of frequency.

**Ground wave or Head wave**

The first arrival predicted by the group velocity curves is often called the ground wave since it has apparently travelled at speed $c_2$. Its path is assumed to be

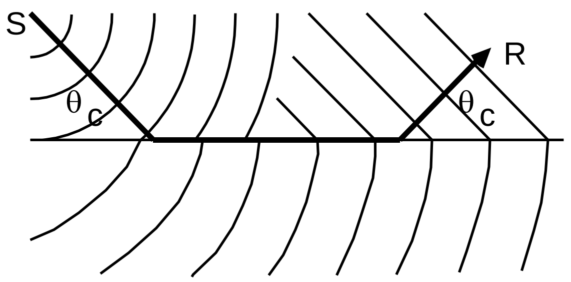


This arrival is usually called the head wave in seismology. It travels down to the boundary at the critical angle, along the interface at the speed of the lower medium and up to the receiver at the critical angle. The waves in the lower medium continually radiate up into the upper medium.

## A Model Experiment

Tolstoy and Clay p 117 describe a model experiment with a source pulse of the form

$$p(t) = A\, t\, e^{-\lambda t} \sin(2\pi f t)$$

with $\lambda = 1.8 \times 10^6\ s^{-1}$ and $f = 5.6 \times 10^5\ s^{-1}$.

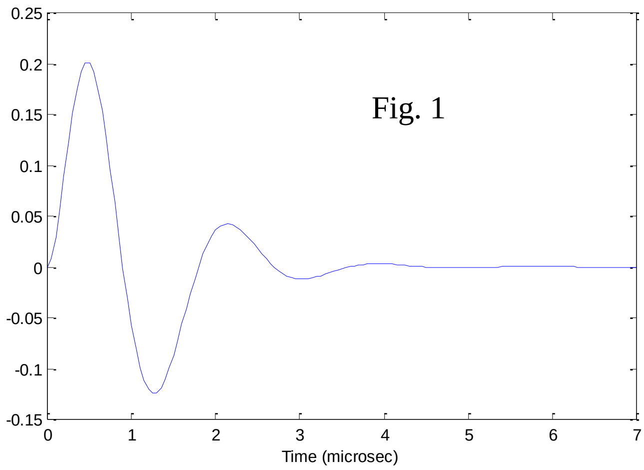


The source pulse is effectively a one cycle pulse at 560 kHz. It has a wide bandwidth with most of the energy in the 280 - 840 kHz band.

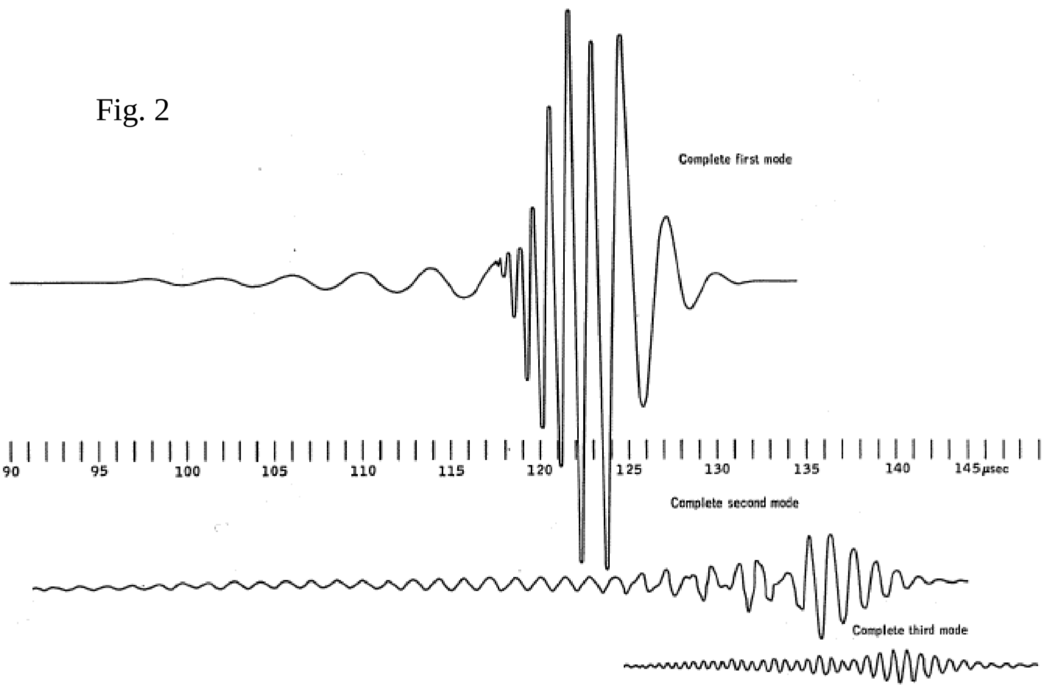


Fig. 4.14 Calculated excitation of three modes for the source of $Q(t) = Ate^{-\lambda t} \sin \omega t,\ t \geq 0$, in the model experiment with two-layer waveguide (Sec. 4.4).

Figure 2 shows the waveforms calculated individually for each mode.

Each waveform begins with a low frequency signal and the frequency gradually increases. Then a high frequency signal arrives and the two combine. The frequencies continue changing smoothly to give a final arrival at a well defined frequency. The initial and final frequencies are different for each mode as expected from the group velocity curves.

Fig. 3

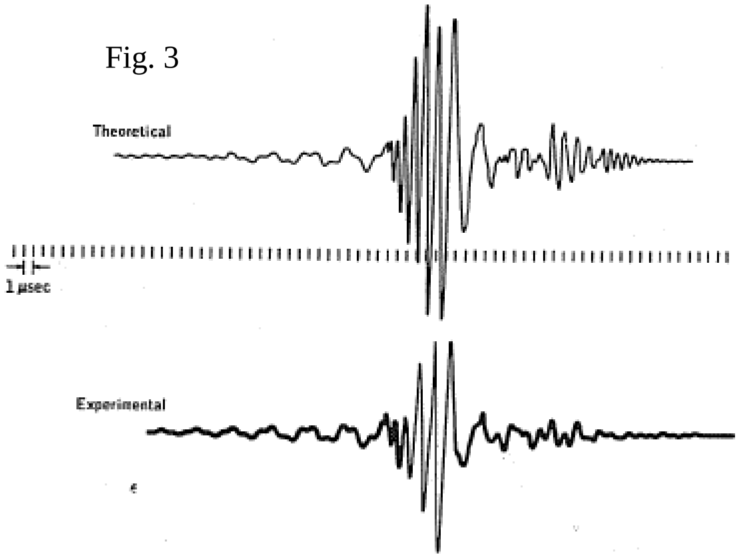


Fig. 4.15 Superposition of the three calculated modes of Fig. 4.14 (theoretical curve) compared with experiment for the two-layer waveguide model.

Figure 3 shows the combined signal and compares it with an experimental waveform for a model experiment with a 2 mm layer of kerosene over salty water.

Fig. 4

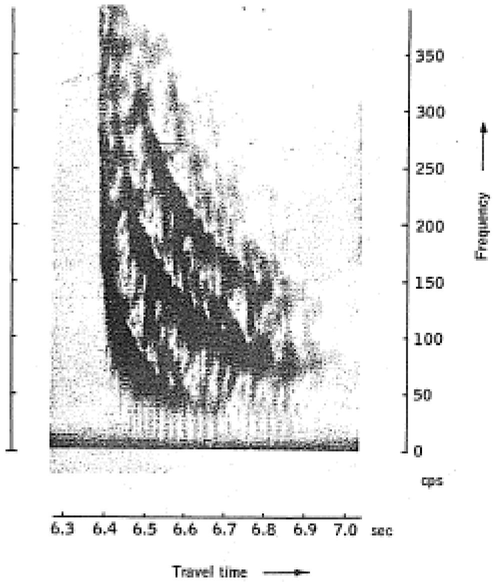


Fig. 4.10 Group-velocity curves displayed by a spectrum analyzer for typical shallow-water shot: 12 kg of TNT at 9.7 km distance in 30 m of water. (Courtesy of J. B. Hersey, Woods Hole Oceanographic Institution.)

Figure 4 shows a frequency time analysis for the signal from an explosive source in shallow water.
The three dark bands beginning at high frequency and ending at low frequency correspond to the first three modes.
Each mode signal begins at high frequency and ends at a well defined low cutoff frequency. Cutoff frequency increases with mode number.
Higher modes have lower group velocity and travel slower (in shallow water).

## Mode extraction

For a narrow band signal the normal mode functions $U_n(z)$ are approximately independent of frequency and we can write

$$p(r,z,t) \approx \sum_{1}^{N} A_n U_n(z) \tag{5.8}$$

where

$$A_n(r,t) \approx [Q/\rho(z_s)]\, e^{i\pi/4} [2\pi/k_n r]^{1/2} U_n(z_s) \int S(\omega) \exp(ik_n r)\, e^{-i\omega t} d\omega \tag{5.9}$$

This parameter $A_n(r,t)$ is the signal associated with each mode and represents a pulse travelling at the mode group velocity.

An experimental waveform for $A_n$ can be extracted from a set of data by multiplying p(r,z,t) on the left by $U_m(z)/\rho(z)$ and integrating over depth. This gives

$$\int [U_m(z)/\rho(z)]\, p(r,z,t)\, dz = \int [U_m(z)/\rho(z)] \sum_{1}^{N} A_n(r,t)\, U_n(z)\, dz = A_m(r,t) \tag{5.10}$$

where the last step follows because the modes are orthogonal.

In practice we sample the field p(r,z,t) at a finite number J of depths $z_j$ and the integration is approximated by

$$\sum_{1}^{J} [U_m(z_j)/\rho]\, p(r,z_j,t) \approx \int [U_m(z)/\rho]\, p(r,z,t)\, dz \approx A_m(r,t) \tag{5.11}$$

This weighted summation of the signals measured at a series of depths enables the waveform associated with each mode to be extracted provided the number of depth samples is greater than the number of modes. The use of the $U_m(z_j)$ as weighting functions in the summation gives quite good separation of the mode signals. A better weighting function using a pseudo inverse matrix [Tindle et al.(1978)] can give almost perfect separation of the mode signals.

**Hauraki Gulf Experiment** (Tindle et al. J. Acoust. Soc. Am. 64, 1178-1185 (1978))

If a narrow bandwidth pulse is transmitted, each normal mode will have its own group velocity. Therefore each mode travels at its own speed and can arrive separated from the other modes.

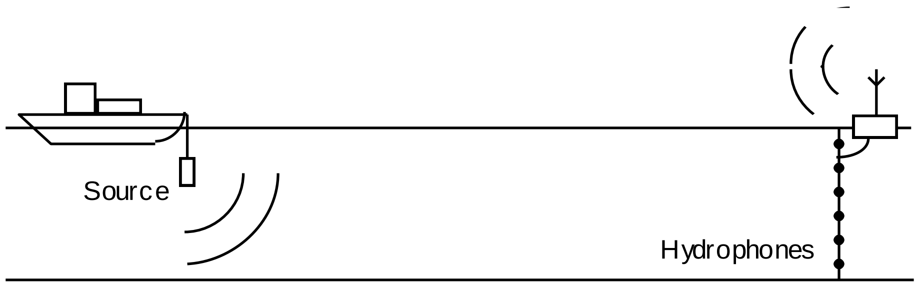


In a shallow water normal mode experiment a sound source transmits to a vertical array of hydrophones. The received signals are transmitted back to the ship and recorded.

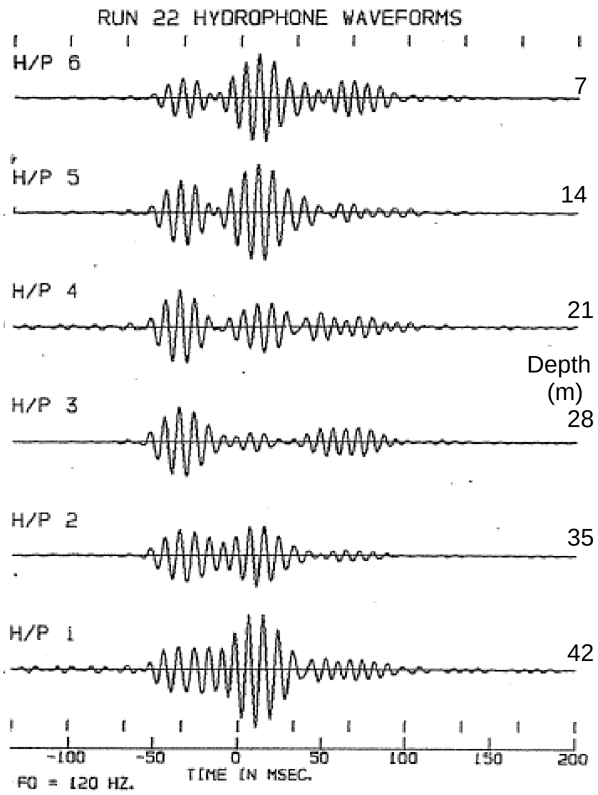


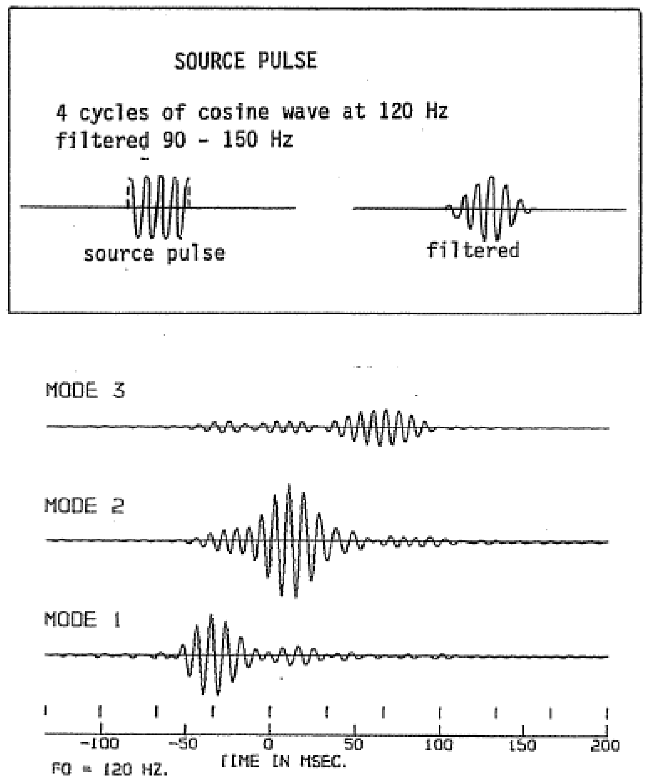


The source transmitted a smoothed four cycle cosine pulse at 120 Hz as shown.

The waveforms on the left were taken on a vertical string of hydrophones, evenly spaced in 50 m water depth at a range of 5 km.

The hydrophone waveforms show the signals received at the various depths as indicated. There are three pulses arriving on most hydrophones.

The first pulse arrival has the depth dependence characteristic of mode 1. It is small near the surface and bottom and larger in the middle of the water column. The first pulse arrival has the same phase at all depths, as can be verified by placing a ruler on the figure.

The second arrival has the depth dependence characteristic of mode 2. It has a null near the middle of the water column and has very small amplitude at 28 m. It has maxima at about 1/4 and 3/4 of the water depth giving large amplitude at 14 m and 42 m. There is a phase reversal at the null and the pulses above the null have the opposite phase from those below the null.

The third arrival is less distinct due to attenuation but has the depth dependence of mode three.

Since the modes have their own value of group velocity they arrive at different times as the results show. The total travel time from the source was about 3.4 seconds.

The results of mode extraction applied to the experimental hydrophone waveforms is shown as the mode waveforms on the right. Summation of the hydrophone signals with the appropriate weightings enhances each mode in turn.

**Theoretical waveforms**

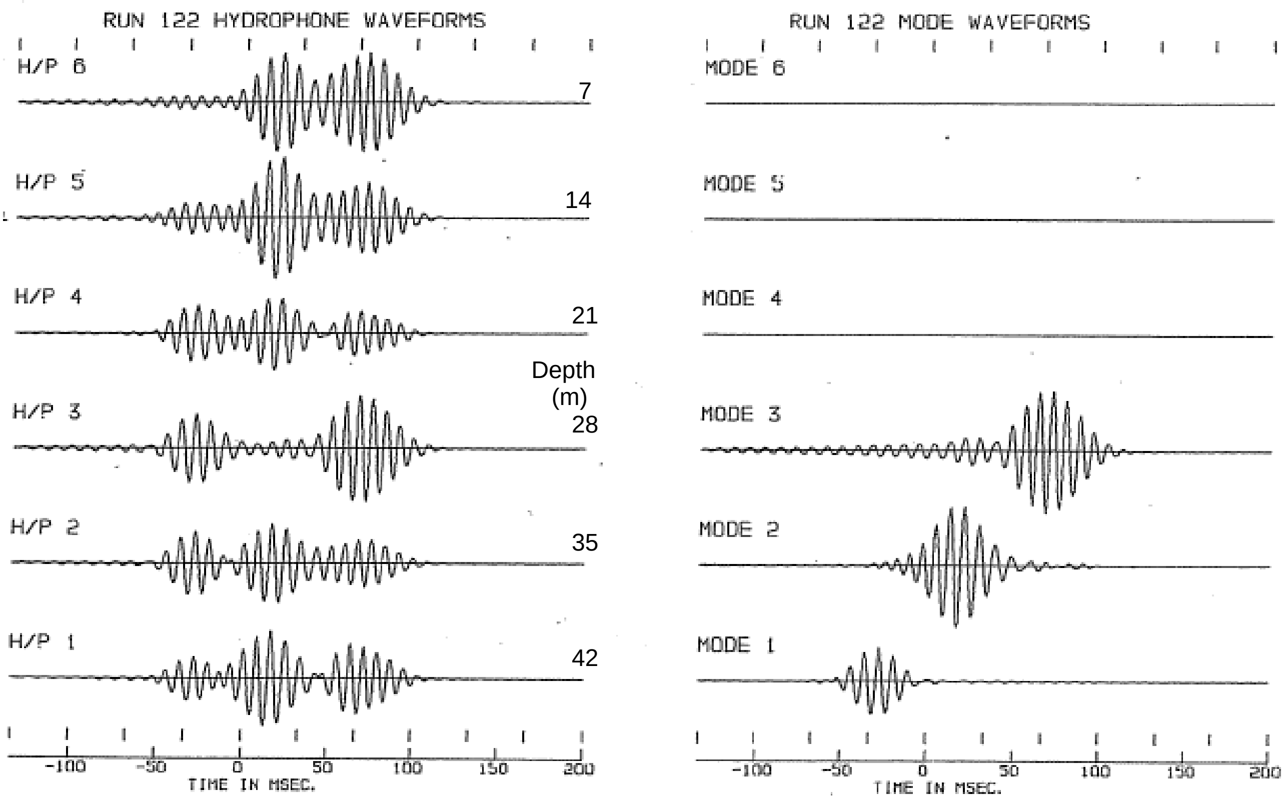


The left figure shows theoretical waveforms corresponding to the Hauraki Gulf experiments. When compared with the experimental waveforms there is excellent agreement of relative arrival times, pulse shapes and mode shapes as a function of depth. The relative mode amplitudes do not agree because attenuation was not included in the theory. The ratio of amplitudes of theory and experiment was used to measure attenuation.

Mode extraction leads to the waveforms on the right. Each mode signal is a replica of the source signal except that there is more dispersion for the higher modes and the pulse becomes lengthened. There is good agreement of waveform shapes and arrival times with the experimental results. Amplitudes do not agree because attenuation has not been included.

## Normal modes in deep water

In deep water the sound speed profile c(z) has a minimum $c_0$ at some depth $z_0$.
The depth equation can be written

$$\frac{d^2Z}{dz^2} + \gamma^2 Z = 0 \tag{5.16}$$

where

$$\gamma^2 = \left( \frac{\omega^2}{c(z)^2} - k^2 \right) \tag{5.17}$$

As before the solution oscillates when $\gamma^2$ is positive and decays exponentially when $\gamma^2$ is negative. However, now the transition between them occurs when $\gamma^2 = 0$ and this can occur within the water at some depth $z_t$. This is referred to as a the turning point for wave number k as the solution changes smoothly between oscillating and exponential behaviour at this point.
The low order modes have two turning points within the water column. The first three modes for a very low frequency are shown in the diagram. They are plotted at their phase velocity.

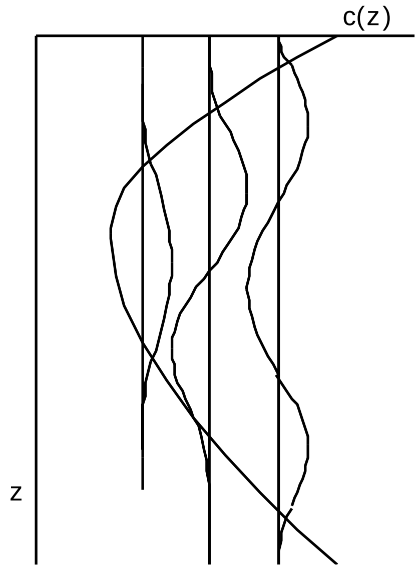


The eigenvalues for these modes are not determined by the boundary conditions. Instead they are determined because the exponential and oscillatory solutions must match smoothly at the turning points. Smooth matching means that both value and derivative must be continuous. For an arbitrary value of k the solutions will usually not match. The value of k is adjusted until a match occurs.

- As before the n-th mode function has n maxima and its own group velocity.
- Each successive mode has turning points further apart in the water column.
- Note that the turning points for a given mode are at the same value of sound speed.

The diagram shows the first three modes at a very low frequency. At a somewhat higher frequency the low order modes shown would move much closer to the sound speed minimum and therefore would have much smaller vertical extent.

## 6. NORMAL MODES AND RAYS

### Modes and Rays

The correspondence between modes and rays can be obtained by considering two sets of wave fronts each making an angle θ with the horizontal.

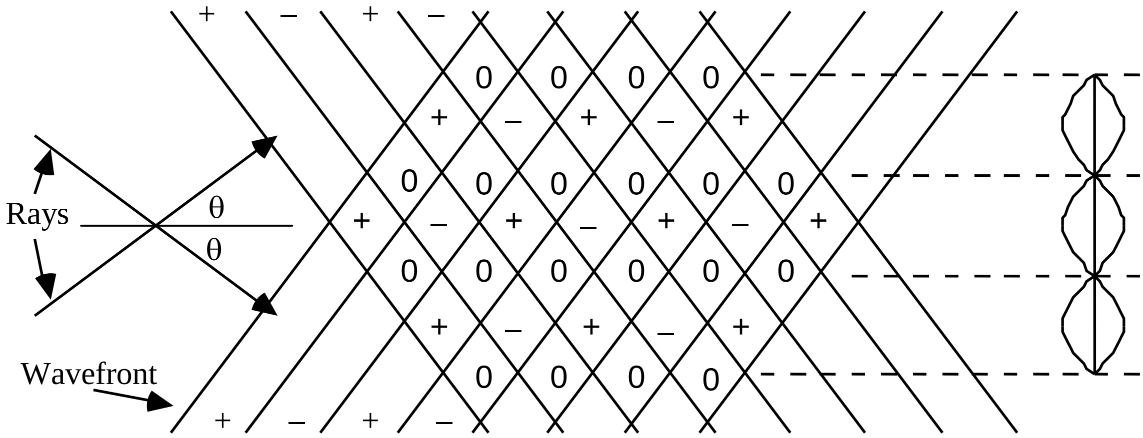


The wave fronts in the figure mark the boundaries between crests (marked +) and troughs (marked –).
Where wavefronts overlap the two sets of wavefronts
either cancel when a crest of one set of waves matches a trough of the other set
or reinforce to produce a larger crest or trough.
As time progresses the wavefronts move in the direction of the rays but the whole pattern appears to move to the right. Therefore the **depth** at which the cancellation takes place stays constant. Thus there are **nodes** at well defined depths.
At depths between the nulls the sound field oscillates between strong maxima and minima. These depths are **antinodes**.
This vertical distribution of energy corresponds to a normal mode pattern as indicated at the right of the figure.

Only wavefronts at certain angles will reinforce because the boundary conditions must also be satisfied. At the surface there must always be a zero of pressure. At the bottom the incident and reflected waves will have a definite phase relationship.
In order to persist the wave pattern must have wavefronts which stay in step after successive reflections at surface and bottom. If they are not in step, successive reflections will lead to eventual cancellation.
Thus wavefronts at certain angles reinforce and form the normal modes.

## Equivalent rays

The rays and normal modes can be related by the requirement that they must have the same vertical separation of nodes.
The diagram shows three wavefronts. The two upgoing wavefronts through A and B are perpendicular to the upgoing ray AD. There is one downgoing wavefront AB.
For simplicity we consider the two upgoing wavefronts to be crests and the downgoing wavefront to be a trough. This means that points A and B are both nulls and the vertical separation of nodes is the distance BC.

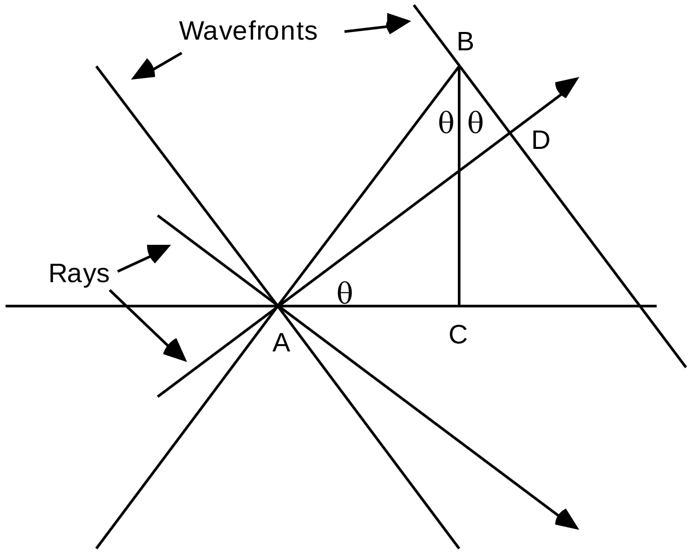


Using geometry we have

$$AD = \lambda \qquad \frac{AD}{AB} = \sin 2\theta \qquad \frac{BC}{AB} = \cos\theta \qquad \Rightarrow \quad BC = \frac{\lambda}{2\sin\theta}$$

We also have

$$\lambda = \frac{c}{f} = \frac{2\pi c}{\omega}$$

Therefore the vertical separation of the nodes of the wavefront pattern is $\dfrac{\pi c}{\omega \sin\theta}$

Since the normal mode function is $\sin(\gamma_n z)$ the vertical distance between nulls of the normal mode pattern is $\dfrac{\pi}{\gamma_n}$ .

Equating these we find

$$\gamma_n = \frac{\omega}{c} \sin\theta \tag{6.1}$$

and using

$$\gamma_n = \left( \frac{\omega^2}{c^2} - k_n^2 \right)^{1/2} \tag{6.2}$$

we have

$$k_n = \frac{\omega}{c} \cos\theta \tag{6.3}$$

Therefore we can draw the following triangle

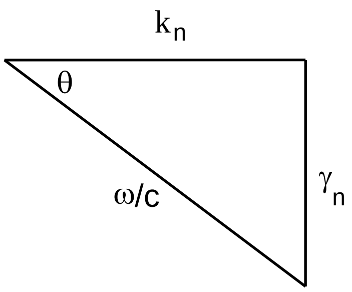


This triangle is very useful in relating rays and modes since $k_n$ and $\gamma_n$ are mode quantities and θ is a ray quantity.
The angle θ is called the angle of the **equivalent ray**.

**Critical angle**
In the Pekeris problem the critical angle $\theta_c$ at the bottom has

$$\cos \theta_c = c_1 / c_2 \qquad (6.4)$$

Discrete normal modes exist for

$$\omega/c_1 > k_n > \omega/c_2$$

i.e. mode cut off is given by

$$k_n = \frac{\omega}{c_2}$$

but using (6.3) this is equivalent to $\frac{\omega}{c_1}\cos\theta = \frac{\omega}{c_2}$ which simplifies to $\cos\theta = c_1/c_2$

Comparing this with Eq. (6.4) shows that the cutoff for discrete modes corresponds to the critical angle for rays. Therefore the energy in the discrete modes corresponds to rays which are totally reflected at the bottom. We conclude that **discrete modes correspond to totally reflected rays**.

Discrete modes are often called trapped modes because their energy is trapped in the water layer. Continuous modes correspond to rays beyond the critical angle which are refracted into the bottom.

**Turning points in deep water**
Even though we have derived the relationship (6.3) for constant c, it holds for variable c(z) also.
In Snell's law cosθ/c was constant. Therefore, using (6.3), $k_n$ is constant and corresponds to the eigenvalue of the mode.
i.e. $k_n$ stays constant while θ and $\gamma_n$ vary.
In particular the ray becomes horizontal for θ = 0 and this corresponds to $\gamma_n = 0$ which we showed earlier was the turning point of the mode function.

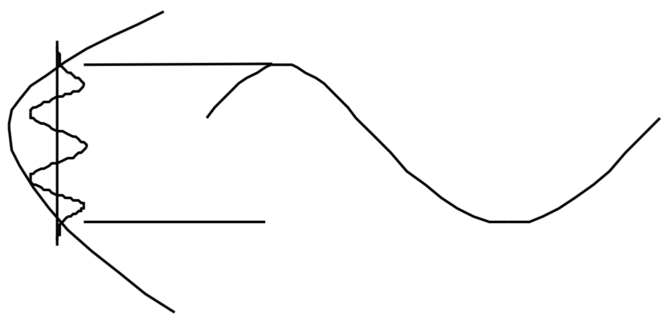

Thus the turning points of the mode and the equivalent ray occur at the same depths!

## WKB solutions

The development of the WKB (named after Wentzel, Kramers and Brioullin) expression for the normal modes gives an approximate but useful phase and amplitude representation of normal modes which will enable us to make a number of connections between normal modes and rays.

The observation that deep water normal modes are functions which oscillate as a function of depth suggests that it should be possible to write

$$U(z) = A(z) \sin[\phi(z)] \qquad (6.5)$$

so that the mode function is replaced by an amplitude function and a phase function. We expect the amplitude function A(z) to be slowly varying with no zeros and we expect the zeros to be given when the phase function $\phi(z)$ passes through multiples of $\pi$.

The depth equation can be written

$$d^2Z/dz^2 + \gamma_n^2 Z = 0 \qquad \text{where } \gamma_n^2 = \omega^2/c^2(z) - k_n^2 \qquad (6.6)$$

We seek a solution of the form

$$Z(z) = A(z) \exp[i\phi(z)] \qquad (6.7)$$

with A(z) a smooth function of position with no zeros. We expect the zeros of Re(Z) to be given by $\phi(z) = (n + {}^1/_2)\pi$.

Substitution and separation of real and imaginary parts gives

$$d^2A/dz^2 - [(d\phi/dz)^2 - \gamma_n^2] A = 0 \qquad (6.8)$$

$$A\, d^2\phi/dz^2 + 2\,(dA/dz)\,(d\phi/dz) = 0 \qquad (6.9)$$

Equation (6.9) has solution

$$A(z) = A_0\,(d\phi/dz)^{-1/2} \qquad (6.10)$$

with $A_0$ constant.

Now assume $d^2A/dz^2 << \gamma_n^2 A$. This is equivalent to assuming that A(z) is slowly varying.

Equation (6.8) becomes

$$d\phi/dz = \pm\gamma_n \qquad (6.11)$$

$$\Rightarrow \quad \phi(z) = \pm \int_a^z \gamma_n(z')\,dz' + \phi_0 \qquad (6.12)$$

Hence combining Eqs. (6.10)-(6.12)

$$Z(z) = A_0 \gamma_n^{-1/2} \exp\left(i[\pm \int_a^z \gamma_n(z')\, dz' + \phi_0]\right) \tag{6.13}$$

or

$$Z(z) = N\, [\gamma(z)]^{-1/2} \sin\left( \int_a^z \gamma(z')\, dz' + \phi_0 \right) \tag{6.14}$$

where N is the normalization and a and $\phi_0$ are constants to be determined.

If a is taken as the upper turning point, detailed consideration of the turning points shows $\phi_0 = \pm \pi/4$.

The WKB solution then becomes

$$Z(z) = N\, [\gamma(z)]^{-1/2} \sin\left( \int_a^z \gamma(z')\, dz' + \pi/4 \right) \tag{6.15}$$

## WKB normal modes

The WKB solution in Eq. (6.15) will be a normal mode solution provided it can be made to satisfy the boundary conditions at the other turning point.

The solution corresponding to (6.15) which is valid at the other turning point (z = b) is

$$Z(z) = N'[\gamma(z)]^{-1/2} \sin\left( \int_b^z \gamma(z')\, dz' - \pi/4 \right) \tag{6.16}$$

and the two solutions (6.15) and (6.16) will be identical provided

$$\int_a^b \gamma(z')\, dz' = (n - \tfrac{1}{2})\, \pi \tag{6.17}$$

i.e.

$$\int_a^b \sqrt{\omega^2/c(z')^2 - k_n^2}\, dz' = (n - \tfrac{1}{2})\, \pi \tag{6.18}$$

Equation (6.18) is therefore an eigenvalue condition for the normal modes, where n is the mode number and $k_n$ is the eigenvalue. [This is equivalent to the Bohr-Sommerfeld approximation to the eigenvalues in Quantum Mechanics.]

The WKB normal mode solution is therefore given by Eq. (6.15) with the eigenvalue given by Eq. (6.18).

**Example**

Consider $d^2Z/dz^2 + \gamma^2 Z = 0$ where $\gamma^2(z) = \omega^2/c^2(z) - k^2$

Let $c^2(z) = c_0^2/(1 - gz)$

giving $\gamma^2(z) = (\omega^2/c_0^2)\,[1 - gz] - k^2$

which is of the form $\gamma^2(z) = \beta^3(a - z)$

Putting $x = \beta(a - z)$ and $U(x) = \beta^2 Z$

gives $d^2U/dx^2 - x\,U = 0$

The solution is the Airy function Ai(–x)

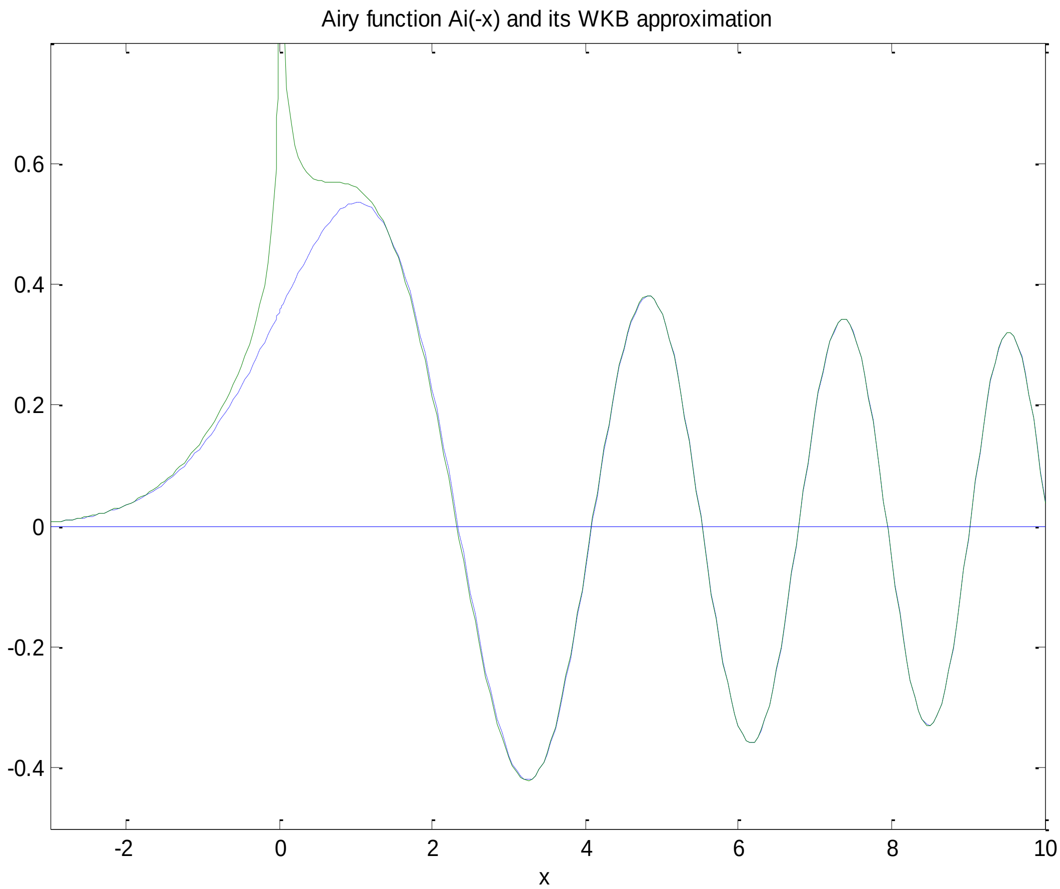


Note

1. The turning point is at $x = 0$ i.e $\gamma(z) = 0$
   exponential decay for $x > 0$ i.e. $\gamma^2 > 0$
   sinusoidal behaviour for $x < 0$ i.e. $\gamma^2 < 0$

2. The wavelength of oscillations decreases as $\gamma^2$ increases.

3 The amplitude decreases as $\gamma^2$ increases. It is large near $\gamma = 0$.
The WKB approximation has infinite amplitude at $\gamma = 0$. The phase remains well behaved.

## Interference of modes

As normal modes propagate they will sometimes interfere to produce maxima and sometimes minima. The WKB approximation to the mode functions expresses the modes in terms of their amplitude and phase and facilitates the study of mode interference.
Consider the normal mode sum

$$p(r,z) \;=\; (\;)\sum_{1}^{N} U_n(z_s)\,U_n(z)\exp(ik_n r) \qquad (6.19)$$

where the empty bracket includes unimportant slowly varying parameters.
Consider terms in n and n+1. Their combined contribution can be written

$$\exp(ik_n r)\left(U_n(z_s)U_n(z) + U_{n+1}(z_s)U_{n+1}(z)e^{i(k_{n+1}-k_n)r}\right) \qquad (6.20)$$

This term is obviously cyclic as the range changes, with a 'mode interference wavelength' $\Lambda$ given by

$$(k_{n+1}-k_n)\Lambda \;=\; 2\pi \qquad (6.21)$$

which can be written using a finite differential as

$$\Lambda \;=\; \frac{2\pi}{\Delta k_n/\Delta n} \qquad (6.22)$$

Since adjacent modes obviously reinforce at the source they also reinforce at multiples of the mode interference wavelength $\Lambda$.

This idea of mode reinforcement can be extended throughout the entire water depth as follows.
Using the WKB approximation for the normal modes and the identity

$$\sin\theta \;=\; \frac{e^{i\theta} - e^{-i\theta}}{2i} \qquad (6.23)$$

we can write the sin function as the difference of exponentials and obtain

$$p(r,z)=(\;)\sum_{1}^{N}\left(\exp i[\int_a^{z_s}\gamma dz'+\pi/4]-\exp[-i(\int_a^{z_s}\gamma dz'+\pi/4)]\right)\left(\exp i[\int_a^{z}\gamma dz'+\pi/4]-\exp[-i(\int_a^{z}\gamma dz'+\pi/4)]\right)$$

$$\times\exp(ik_n r) \qquad (6.24)$$

Now consider the phase $\phi$ of the first term of this expansion. We have

$$\phi \;=\; \int_a^{z_s}\gamma dz' \;+\; \int_a^{z}\gamma dz' \;+\; k_n r + \pi/2 \qquad (6.25)$$

with the explicit form for $\gamma$ this can be written

$$\phi = \int_{z_s\sim}^{z} \left(\omega^2/c(z')^2 - k_n^2\right)^{1/2} dz' + k_n r + \pi/2 \tag{6.26}$$

where the notation $z_s\sim$ means the sum of the integrals from $z_s$ to z via the appropriate turning points, one upper turning point in this case.

Adjacent terms of the integral (i.e. terms in n and n+1) will be in phase when a change from n to n+1 produces a phase change of a multiple of $2\pi$. This will occur when

$$\frac{\Delta\phi}{\Delta n} = 2m\pi \quad \text{where m is an integer.} \tag{6.27}$$

Taking a finite derivative of (6.26) with respect to n gives

$$\Delta\phi/\Delta n = \int_{z_s\sim}^{z} (^1/_2)\left(\omega^2/c(z')^2 - k_n^2\right)^{-1/2} 2k_n\,(\Delta k_n/\Delta n) dz' + (\Delta k_n/\Delta n)\, r$$

Setting this equal to $2m\pi$ and rearranging we find

$$r = \int_{z_s\sim}^{z} \left(\frac{\omega^2}{c^2(z')\, k_n^2} - 1\right)^{-1/2} dz' + \frac{2m\pi}{\Delta k_n/\Delta n} \tag{6.28}$$

Now consider the ray path equation for a ray which has travelled from source to receiver with m complete cycles and one extra upper turning point. The ray path equation is

$$r = \int_{z_s\sim}^{z} \left(\frac{c_0^2}{c(z')^2 \cos^2\theta_0} - 1\right)^{-1/2} dz' + mD \tag{6.29}$$

where D is the cycle distance.

Comparing equations (6.28) and 6.29) we see that they will be identical provided

$$k_n = \frac{\omega}{c_0} \cos\theta_0 \tag{6.30}$$

and

$$D = \frac{2\pi}{\Delta k_n/\Delta n} \tag{6.31}$$

The first of these requirements is well known and relates the horizontal wave number of the mode to the angle of the equivalent ray. The second shows that the ray cycle distance is the same as the mode interference wavelength discussed above.

We conclude that the interference of the modes has produced an interference maximum which follows the ray path of the equivalent ray.

The four possible sign combinations in the terms of (6.33) correspond to the four possible eigenrays for a given number of complete cycles.

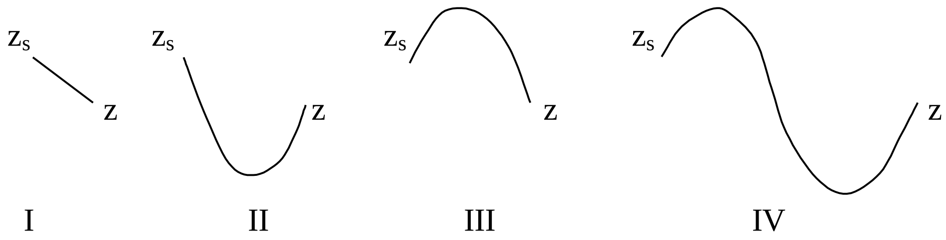


Equation (6.34) corresponds to case III i.e $\int_a^{z_s} \gamma \, dz + \int_a^{z} \gamma \, dz$ .

If the field due to a group of adjacent modes is calculated it has well defined interference maxima. These maxima are plotted as the dots in the figure [from Tindle and Guthrie, J. Sound Vib. (1974)]. The solid line is a ray trace for the equivalent ray for the central mode of the group.

It is clear that adjacent modes interfere to produce energy which follows the ray path of the equivalent ray.

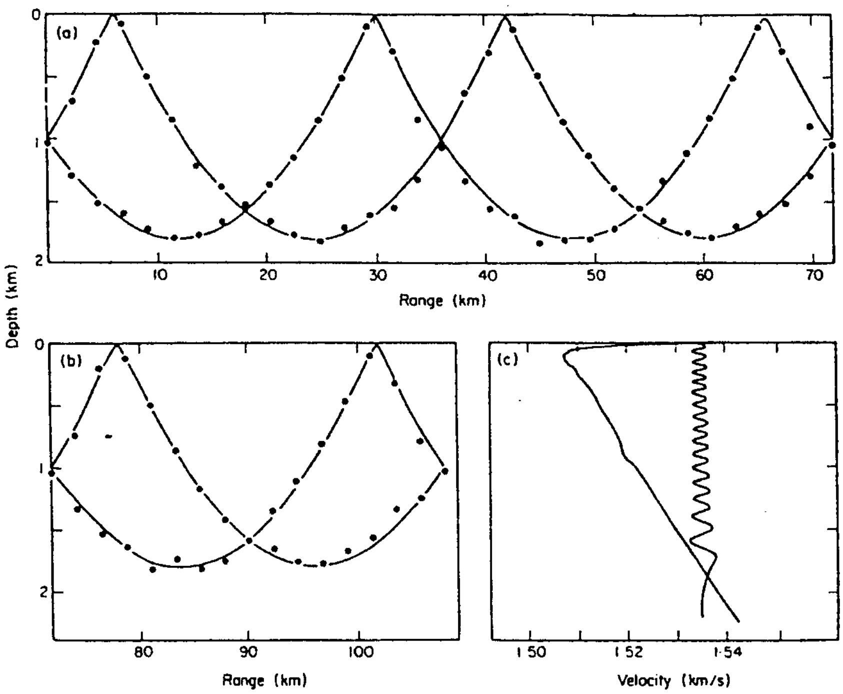


Figure (a) and (b) The dots show the depths of the peaks of the pressure envelopes as a function of range for modes 26 to 34 at 100 Hz. The solid line is a ray trace for the ray equivalent to mode 30. (c) The velocity profile [11] with mode 30 (in arbitrary units) superimposed at the correct phase velocity.

**Modes and Equivalent Rays**

The example below shows a sound speed which drops linearly from 1545 m/s at the surface to 1490 at mid water depth and then is constant in the lower half of the water column. The frequency considered gives 6 trapped modes.

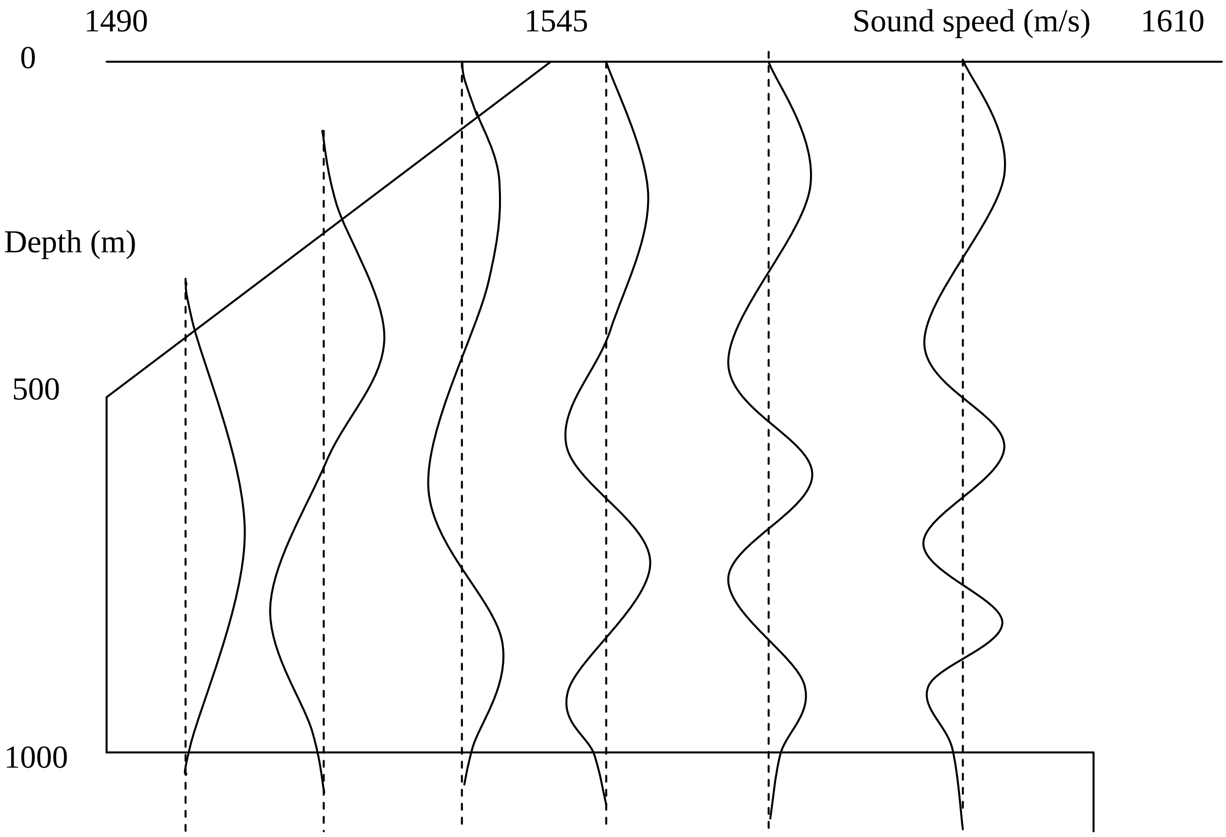


**Equivalent rays for modes 1 to 6.**

Mode eigenvalues and equivalent ray grazing angles are related by $k_n = [\omega/c(z)] \cos\theta(z)$.
The lowest mode has lowest phase velocity and highest k, hence lowest grazing angle.

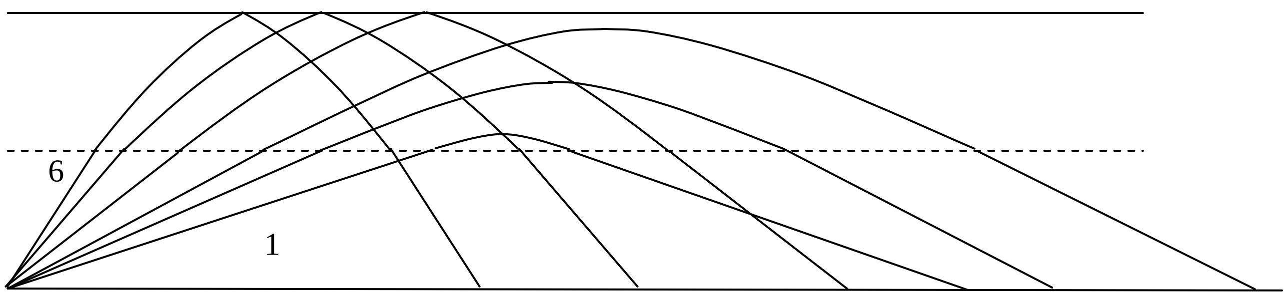


A source in the lower half will excite all modes (unless it is on a null).
Mode 3 will arrive first because the equivalent ray spends longer in the higher speed layer and has the longest cycle distance.
Arrival order will probably be 3, 2, 1, 4, 5, 6 i.e. order of decreasing cycle distances.
A receiver near the surface will not receive modes 1-2.

## 7. BEAM DISPLACEMENT

**Beam Displacement on Reflection** (Brekhovskikh Ch 14)

Consider a downgoing plane wave incident on the bottom. The pressure can be represented by

$$p_{inc} = A \exp[i(kr + \gamma z)]$$

where $k = (\omega/c)\cos\theta$ and $\gamma = (\omega/c)\sin\theta$

and $\theta$ is the grazing angle of the ray.

An upgoing reflected wave is given by

$$p_{refl} = B \exp[i(kr - \gamma z)]$$

where B is to be determined.

At the bottom at z = H we have

$$p_{inc} = A \exp[i(kr + \gamma H)]$$

The reflected wave at the bottom is the incident wave multiplied by the reflection coefficient R(k) giving

$$p_{refl} = A\, R(k) \exp(2i\gamma H) \exp[i(kr - \gamma z)]$$

Now construct a beam by taking a narrow range of angles

$$p_{inc} = \int A(k) \exp[i(kr + \gamma z)]\, dk$$

with A(k) strongly peaked at $k = k_0$.

$$p_{refl} = \int A(k)\, R(k) \exp(2i\gamma H) \exp[i(kr - \gamma z)]\, dk$$

Now if $R(k) = |R(k)| \exp[i\phi(k)]$ and $|R(k)|$ is slowly varying we can approximate $\phi(k)$ as

$$\phi(k) \approx \phi(k_0) + (k - k_0)(d\phi/dk)$$

At the bottom

$$p_{inc}(r,H) = \int A(k) \exp[i(kr+\gamma H)]\, dk \qquad (7.1)$$

$$p_{refl}(r,H) = \int A(k)\, |R(k_0)| \exp\big(i[\phi(k_0)+(k-k_0)(d\phi/dk)]\big) \exp(2i\gamma H) \exp[i(kr-\gamma H)]\, dk$$

$$\Rightarrow\ p_{refl}(r,H) = R(k_0) \exp[-ik_0(d\phi/dk)] \int A(k) \exp\big(i[k(r+d\phi/dk)+\gamma H]\big)\, dk \qquad (7.2)$$

Comparing (7.1) and (7.2) shows the reflected beam is the incident beam multiplied by the reflection coefficient $R(k_0)$, phase shifted by $-k_0(d\phi/dk)$ and shifted along the boundary by the beam displacement Δ where

$$\Delta = -(d\phi/dk) \qquad (7.3)$$

The beam displacement arises when the phase change on reflection is a function of angle of incidence and can be seen geometrically in the diagram.

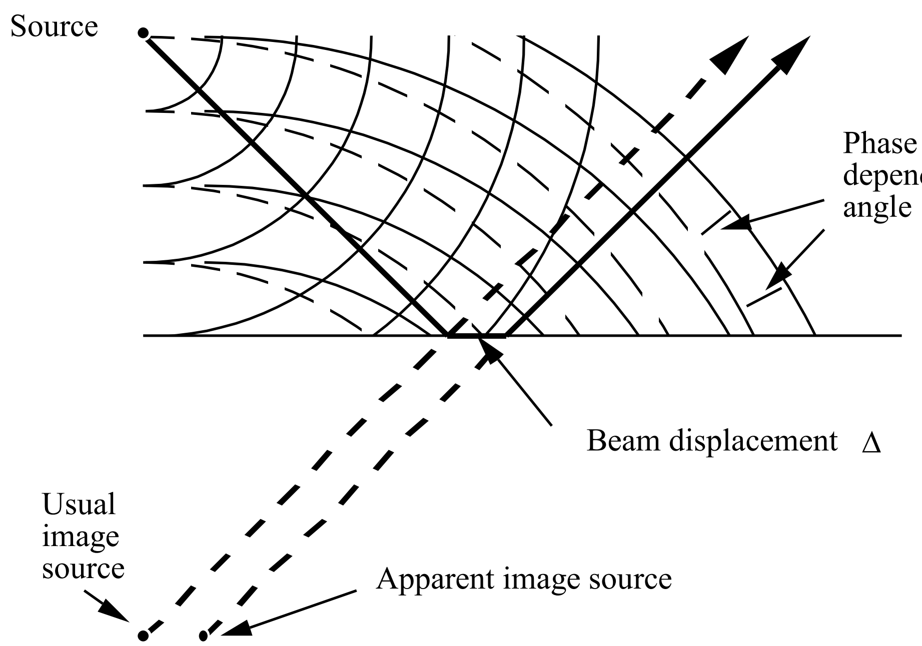


The source emits circular wavefronts as shown.

The usual reflected wavefronts are shown as dashed curves and appear to come from the usual image source. The usual image source is at the source position reflected in the interface.

Because the phase change on reflection is a function of angle the reflected wavefronts are displaced from the usual wavefronts and are shown as solid curves.

The displaced wavefronts have an apparent image source which is displaced as shown from the usual image source.

The path of a representative ray is shown. It appears to come from the image source and the ray path appears to have a lateral shift at the interface.

Using $k = (\omega/c)\cos\theta$ the beam displacement can be found in terms of angles as

$$\Delta = -\frac{d\phi}{d\theta}\frac{d\theta}{dk} = \frac{c}{\omega\sin\theta}\frac{d\phi}{d\theta} \qquad (7.4)$$

Inclusion of beam displacement is important in ray calculations of the sound field at low frequencies in shallow water. Eigenray angles are found using ray paths which include beam displacement.

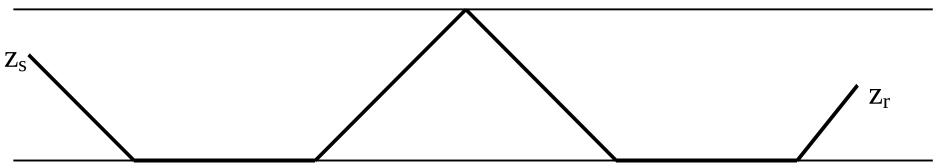


With inclusion of beam displacement ray calculations agree with normal mode calculations and experimental data. [Tindle and Bold, J. Acoust. Soc. Am. **70**, 813-819 (1981) and Tindle, **73**, 1581-1586 (1983)]

The parameters used were

| | | | |
|---|---|---|---|
| $c_1$ = 1508 m/s | $c_2$ = 1605 m/s | $\rho_2/\rho_1$ = 1.25 | H = 50 m |
| $z_0$ = 6 m | z = 7 m | r = 5100 m | f = 140 Hz |

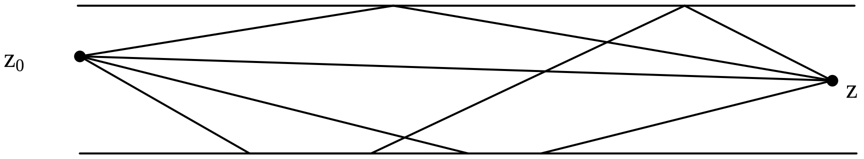


About 50 eigenrays with beam displacement contribute to the signal at the receiver.

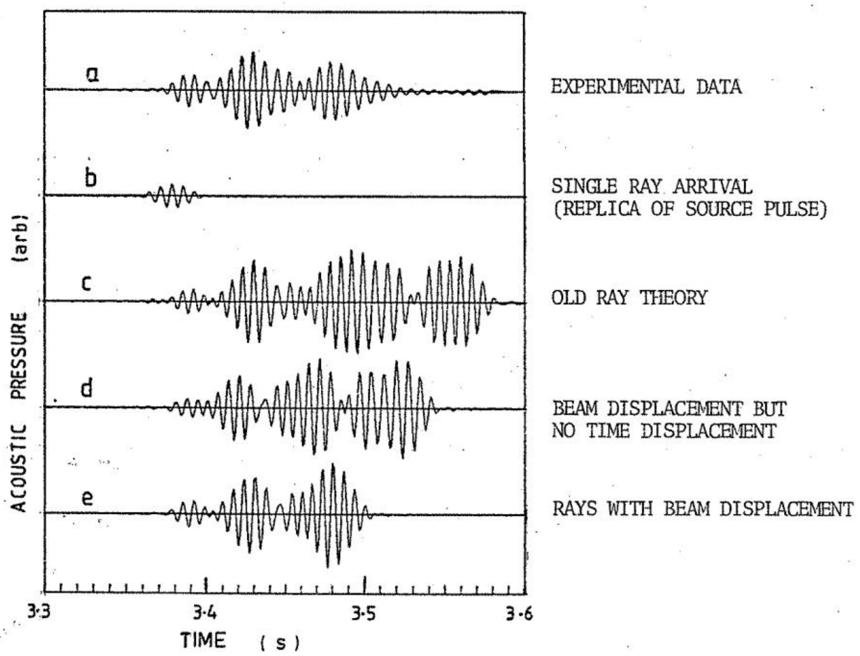


Waveform a shows distinct pulses corresponding to modes 1, 2, 3 arriving in order.

Waveform b is the direct pulse from the receiver. It cancels with the surface reflection as do other low grazing angle paths. Mode 1 begins about 2 cycles (140 ms) later.

Inclusion of beam displacement is necessary to get agreement of mode pulse shapes and travel times. Amplitudes to not agree because attenuation has not been included.

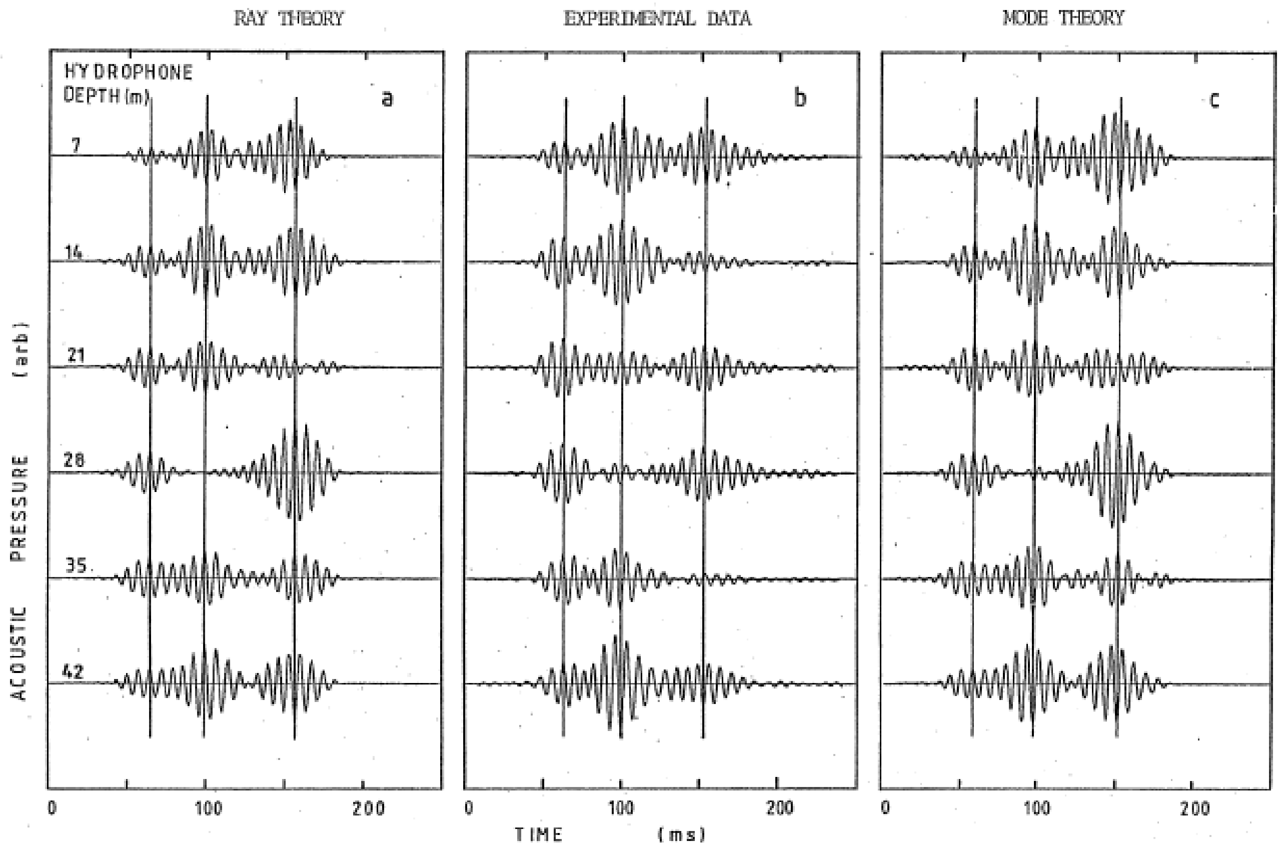


The waveforms on all six hydrophones are shown in the figure.

There is good agreement of waveforms between ray and mode theoretical results. Both agree well with pulse shapes and arrival times of modes. As before, amplitudes do not agree because attenuation has not been included.

## 8. APPLICATIONS

### Tomography

Underwater acoustics is now used for tomography and large scale measurement of ocean parameters. The speed of sound in the ocean depends only on salinity, pressure and temperature. In the ocean salinity is constant, pressure is a simple function of depth so sound speed changes are due only to temperature changes.

The upper figure shows the high angle eigenrays for a source and receiver 300 km apart in the sound speed profile on the left. There are many eigenrays which cycle close to the sound speed minimum but only one is shown. The others have have been omitted for clarity.

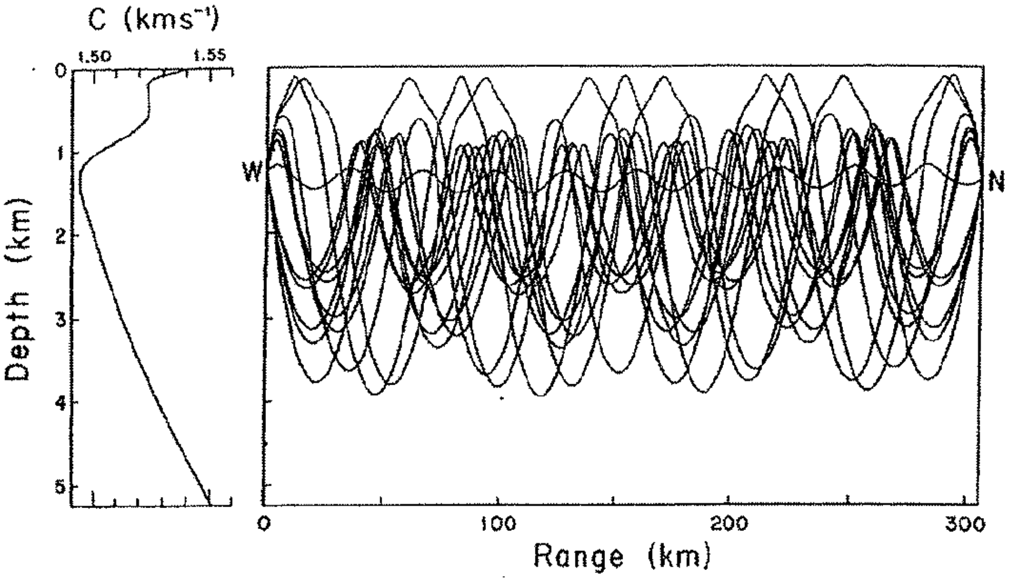


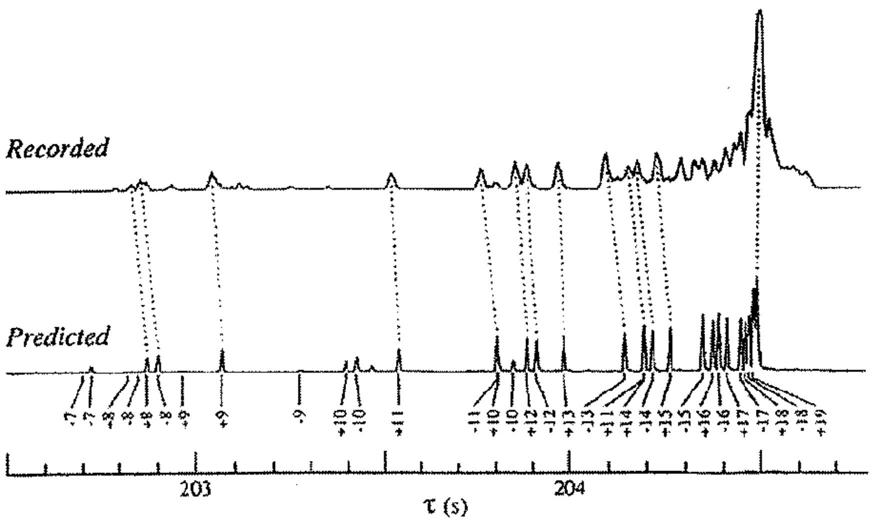


The lower figure shows the recorded and modelled signal intensity as a function of time.

The early arrivals correspond to the high angle rays which have maximum depth variation. These rays spend the majority of their time at higher speed and arrive first.

Rays with lower launch angles have less depth variation and cluster around the sound speed minimum. They travel more slowly and arrive as a bunch in a final crescendo.

Long term monitoring of the travel time of the early arrivals can be used for ocean tomography. If a patch of warmer water develops near the surface then rays which pass through that patch will arrive earlier than before. The travel time variations can be inverted to map ocean temperature changes.

**Vertical Line Array (VLA)**

A basic tool in underwater acoustics is a vertical line array of hydrophones. The hydrophones are usually uniformly spaced.

Typical theoretical and experimental deep water receptions are shown in the figure. The data is for a range of 1000 km and a source at 250 Hz. The array was 3000 m long with 50 hydrophones at 60 m intervals.

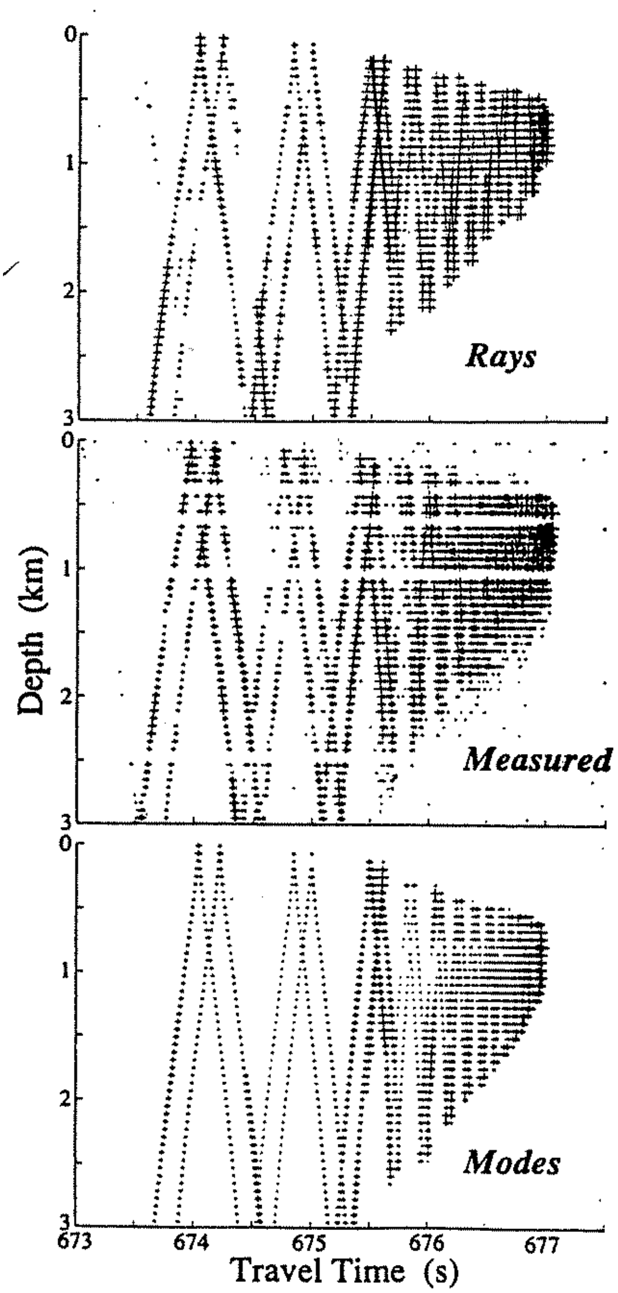


The middle panel is data. The top and bottom panels are modelled using rays and modes respectively in the average sound speed profile.

The early arrivals are discrete and correspond to wavefronts of rays with turning points far from the sound speed minimum. The first arrival is an upgoing ray wavefront because it arrives first at the deeper hydrophones.

The later arrivals have many overlapping upwards and downwards rays and form the low order normal modes near the sound speed minimum.

## Wavefronts

If rays are traced for a fixed time they form a wavefront (also called a time front).
Turning points in the ray path lead to folds in the wavefront. The ends of the folds are caustics and mark the edge of the geometric shadow. The figure shows the ray trace and the time front for a source in a Munk sound speed profile. The limiting angle for the ray trace is the angle for rays which just graze the surface. The timefront is shown at a 54.9 s after the wavefront has travelled just over 80 km.

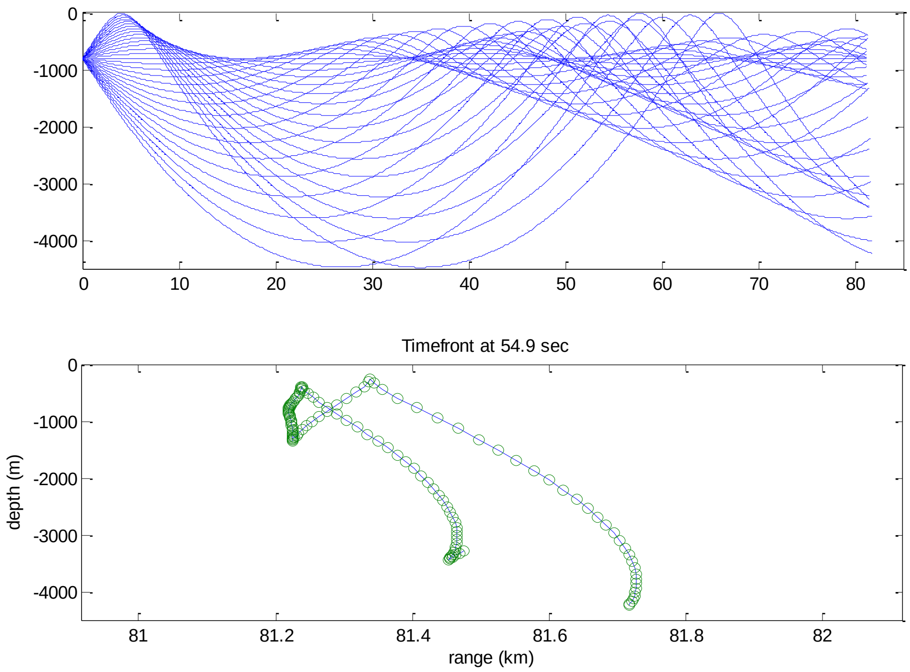


If the wavefront passes a vertical array the time order is reversed as in the left diagram below.

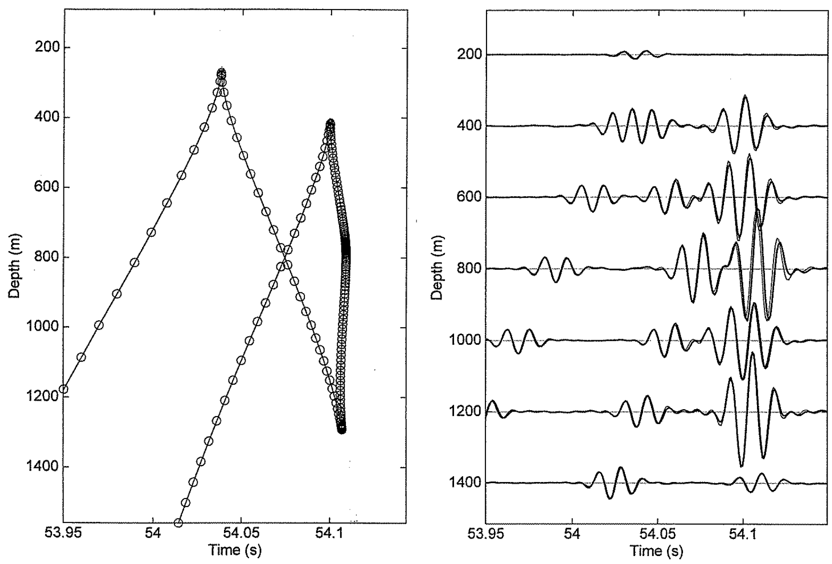


The right figure above shows the waveforms that would be measured if the source emitted a two cycle pulse at 75 Hz. The modelled waveforms include pulses in the geometric shadow. [Tindle JASA 112, 464-475 (2002)]